ACOUSTIC IMAGING USING BISPECTRAL HOLOGRAPHY

A Thesis
Submitted in Partial Fulfilment of the Requirements
for the Degree of
MASTER OF TECHNOLOGY

By

B. R. K. REDDY

to the
DEPARTMENT OF ELECTRICAL ENGINEERING
INDIAN INSTITUTE OF TECHNOLOGY, KANPUR
AUGUST, 1980

ACOUSTIC IMAGING USING BISPECTRAL HOLOGRAPHY

A Thesis
Submitted in Partial Fulfilment of the Requirements
for the Degree of
MASTER OF TECHNOLOGY

By

B. R. K. REDDY

to the
DEPARTMENT OF ELECTRICAL ENGINEERING
INDIAN INSTITUTE OF TECHNOLOGY, KANPUR
AUGUST, 1980

EE-1980-M-RED-ACO

CERTIFICATE

This is to certify that the thesis entitled, 'Acoustic Imaging using Bispectral Holography' is a record of the work carried out under my supervision and that it has not been submitted elsewhere for a degree.

August 1980

Dr. S.K. Mullick
Professor
Department of Electrical Engineering
Indian Institute of Technology
Kanpur

ACKNOWLEDGEMENT

I wish to express my profound gratitude to Dr. S.K. Mullick who introduced me to this field, and for his constant guidance and inspiration. I am greatly indebted to him for the invaluable encouragement and help given throughout my course of study. My association with him has been fruitful as well as memorable.

I would like to thank my friends Mr. R.V. Chalam and Mr. N. Gopinath, who helped me in the preparation of this report.

Thanks are due to Mr. K.N. Tewari for his neat and efficient typing of this thesis.

Kanpur B.R.K. Reddy

August 1980.

CONTENTS

ABSTRACT

In this report our main concern is Image reconstruction of the object, emitting acoustic signals, using bispectral holography. Recording of the hologram using conventional techniques as well as using bispectral analysis is given. Conventional method is employed for image reconstruction from the recovered hologram signal. The bispectral holographic imaging technique has the potential theoretical advantages of ideal recovery in the presence of noise and distorting medium. Computer simulation of this processing strategy carried out in this work confirms this.

CHAPTER 1

INTRODUCTION

Holography is a technique, meant for the purpose of recording and displaying an image in its true three-dimensional format. It is a synthesis of two branches of optics, namely, interferometry used in recording the hologram, and diffraction used to display the image. This technique of photography has come to be known as holography after the word 'hologram' coined by Gabor to describe the interferogram that is used to record the wavefront to be reconstructed. The initiation for this synthesis came from engineers and physicists working in the area of communications. In communications the analogies to interference and diffraction are respectively modulation and demodulation. It is obvious from this analogy that the information stored in an interference pattern (modulation) can be retreived as a result of diffraction of light by the recorded interference pattern (demodulation).

In the following section a simplified discussion of holography based on interference and diffraction is undertaken. At first, the interference phenomena is studied. As shown in Fig. 1.1, a plane monochromatic wave is split into two equal amplitude plane waves which then traverse separate paths until they are recombined. If the mirrors and beam splitters are perfect and if the optical path lengths are equal, the

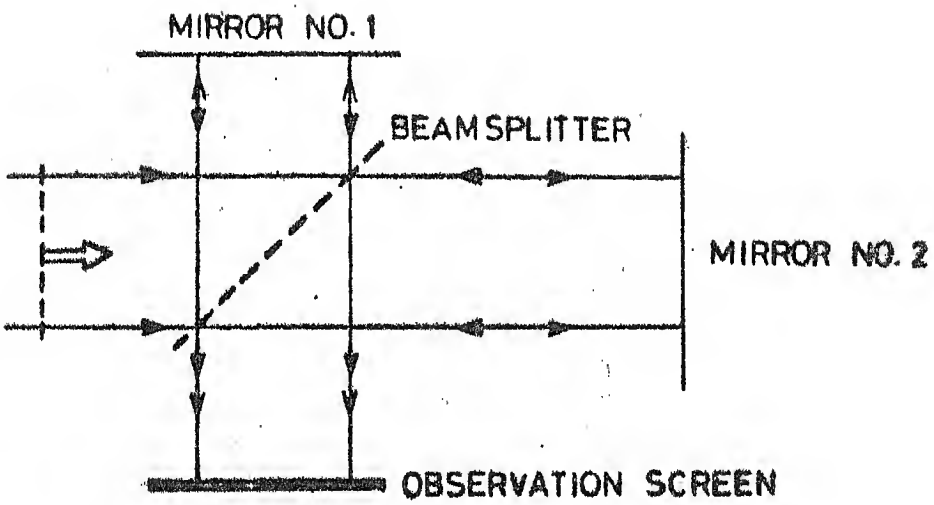

FIG .1·1 MICHELSON INTERFEROMETER

output beam will be exactly like the input beam except for the loss in beam encountered at the beam splitter. A screen placed in the beam will therefore show uniform intensity.

If one of the mirrors is not quite parallel to the wavefront due to a misalignment, the reflected wave from it will combine with the other beam to form a linear system of fringes as shown in Fig. 1.2. Destructive interference occurs wherever the path length difference between the wavefronts is an odd multiple of half the wavelength.

If one of the mirrors is replaced with a concave parabolic reflector, the interference pattern we would expect to see is shown in Fig. 1.3. Note that this ring pattern shows decreasing spacing with increasing distance from the centre. This type of pattern is called Fresnel Zone pattern. If we impart a tilt to the spherical wave, we obtain a partial Fresnel Zone pattern as shown in Fig. 1.4.

When an aperture of some kind is interposed in a collimated beam of light, one might expect to see on the screen, a pattern of light sharply defined by the shadow of the aperture. Looking closely, however, the observer notes that some light exists in the shadow zone. The study of this phenomena is known as diffraction theory. The essense of the theory known as Huygens' principle is that each point on a wavefront can be considered as an elementary point radiating a spherical wavefront. When the elementary

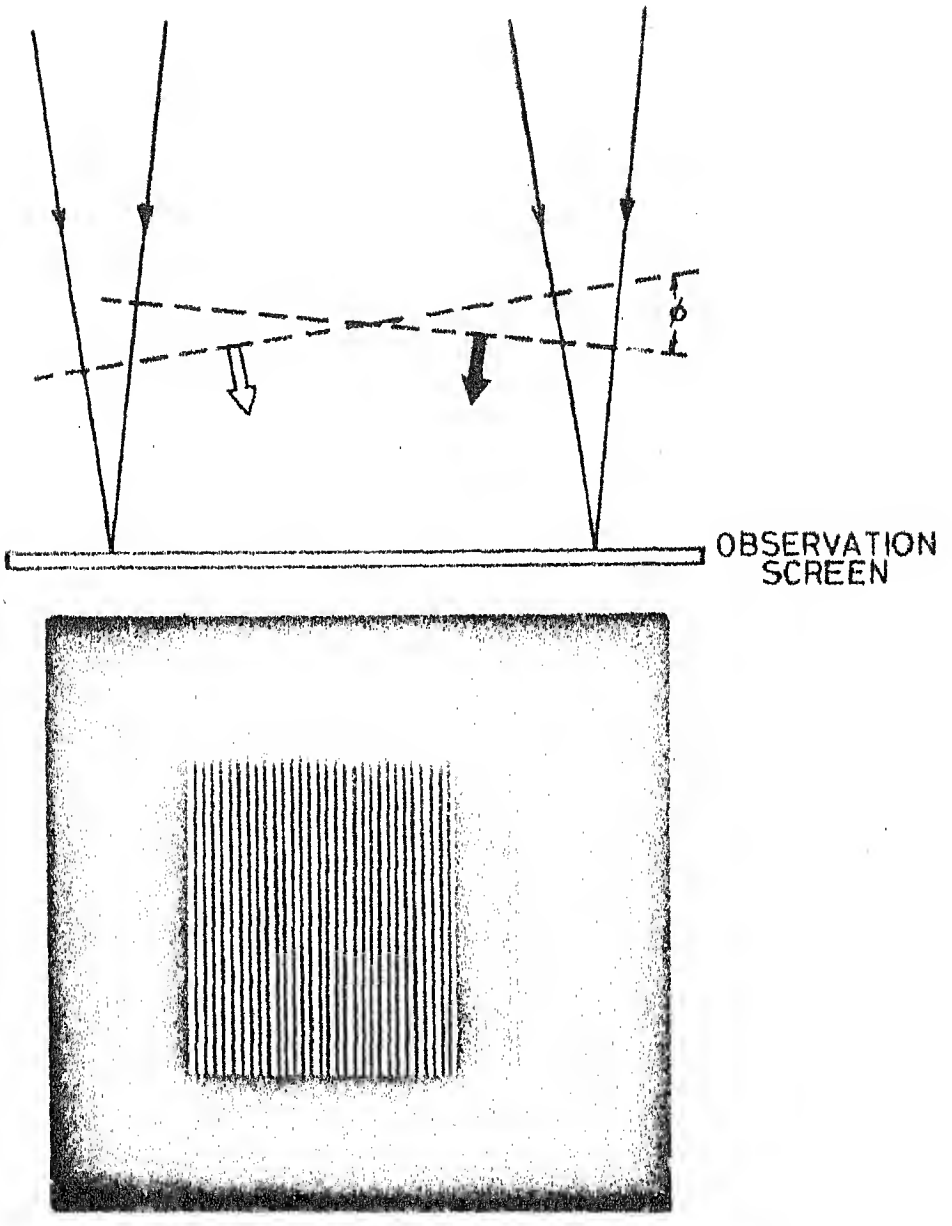

FIG.1·2 INTERFERENCE PATTERN OF TWO PLANE WAVES

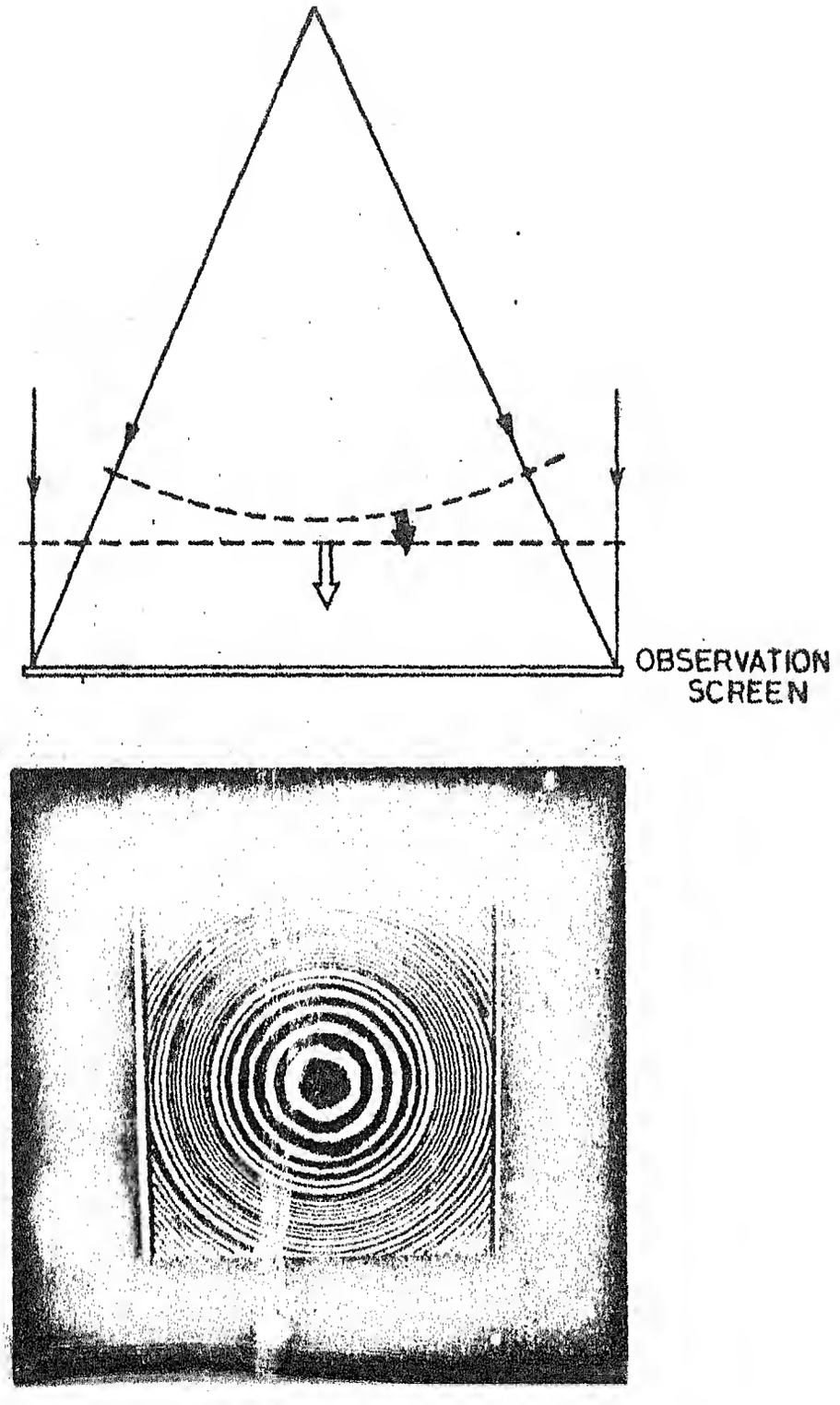

FIG·1·3 FRESNEL ZONE PATTERN

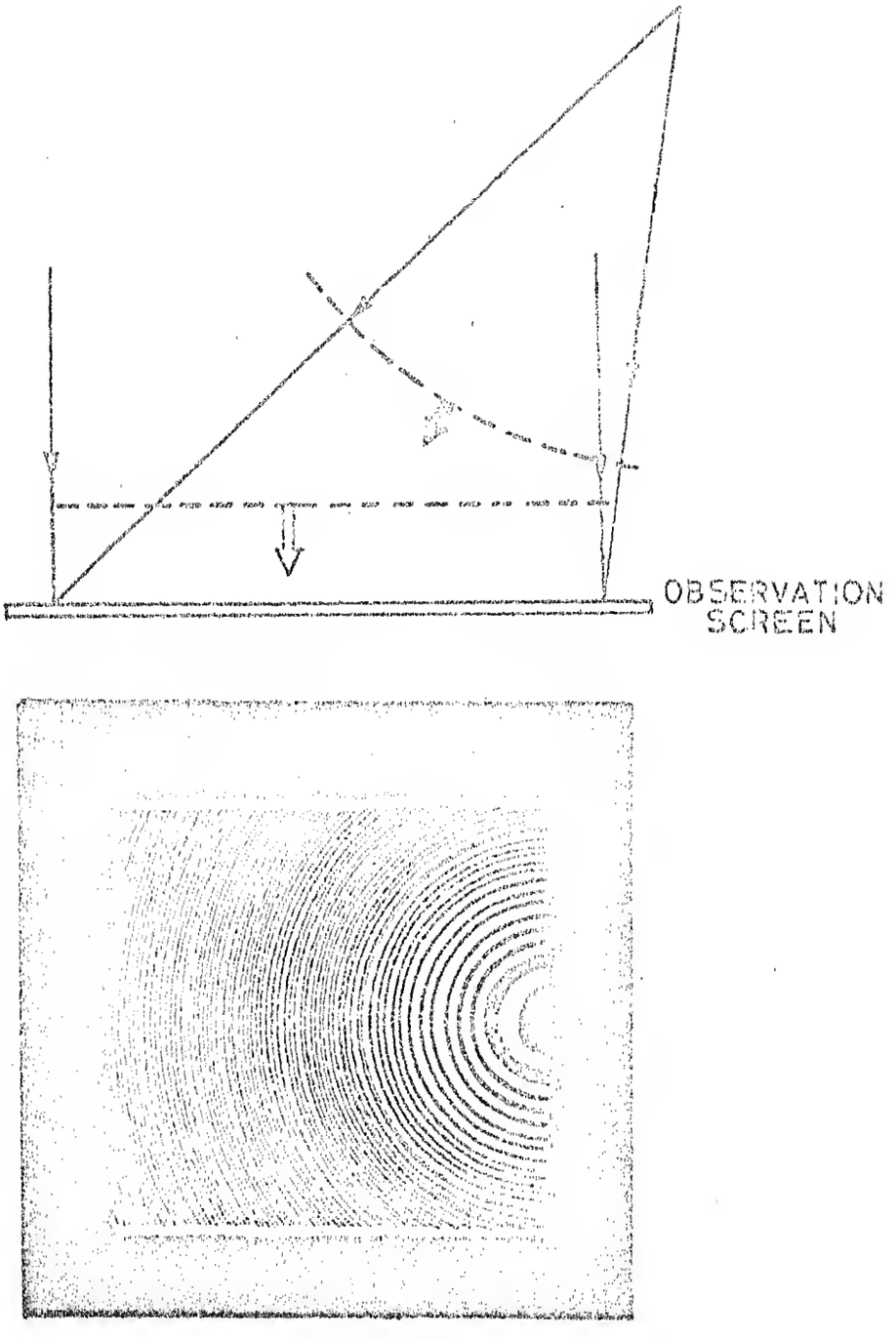

FIG.1·4 OFFSET FRESNEL ZONE PATTERN

wavelets are summoned in the prescribed manner the result is identical to the actual wavefront farther down stream. This principle is useful in analyzing the behaviour of the light in the presence of various types of apertures and obstructions.

A film containing the binary interference pattern generated in Fig. 1.2 is placed in the path of a collimated monochromatic light beam as shown in Fig. 1.5. In this figure we consider a single wavelet in the centre of each transparent space. Note that each circle represents an equiphase surface advanced in phase by 2π from its neighbour to the left. The spatial separation of each surface from the next is one wavelength λ. We can draw a plane phase front tangent to the elementary wavelet phasefronts, three of which are shown in Fig. 1.5. For the binary pattern we can draw many more plane wavefronts at ever increasing angles. Comparing Fig. 1.5 with Fig.1.2, we see that we have reconstructed the beams that made the interference pattern in the first place, with one exception; we have an extra beam at the conjugate angle.

The second example of the interference pattern was the Fresnel Zone pattern (Fig. 1.3). Fig. 1.6 shows what happens when this is illuminated. The Fresnel Zone pattern is, in effect, a locally linear grating, acting much the same way as our first example, except that the spacing varies as described previously. Hence the locally diffracted light changes in direction and the total effect provides a spherical

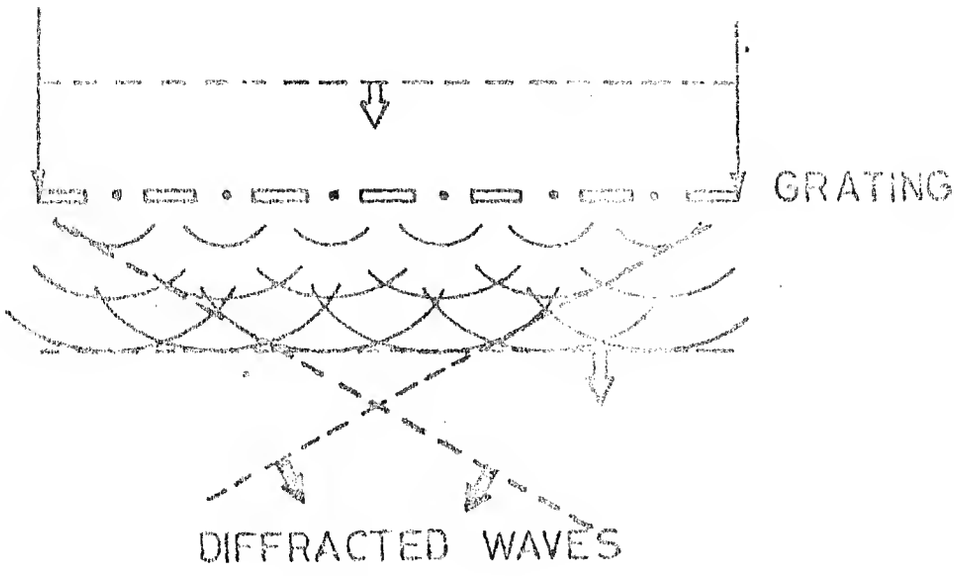

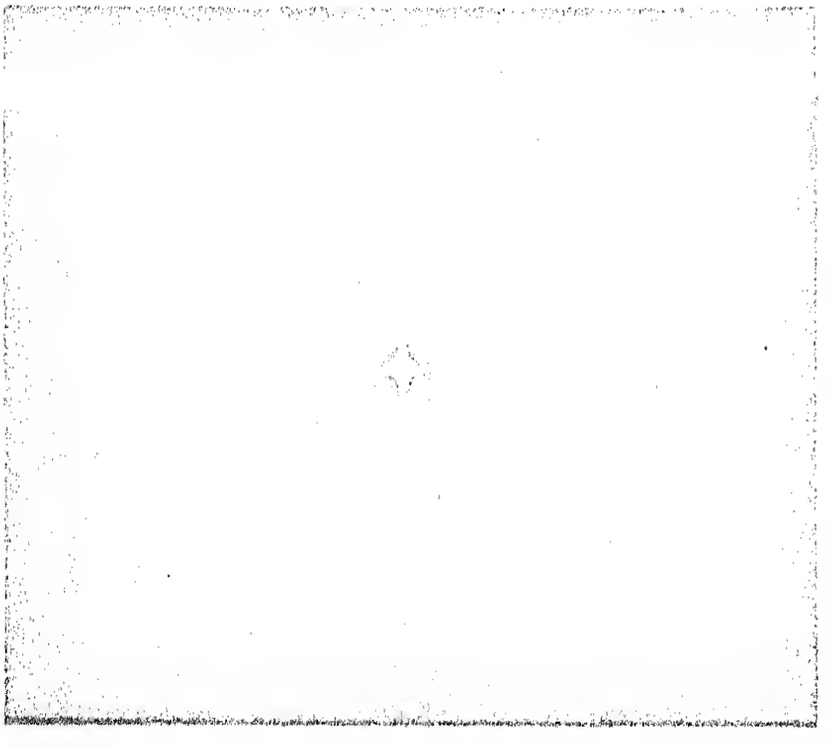

FIG. 1·5 RECONSTRUCTION OF THE PLANE WAVES THAT MADE THE INTERFERENCE PATTERN IN FIG. 1·2

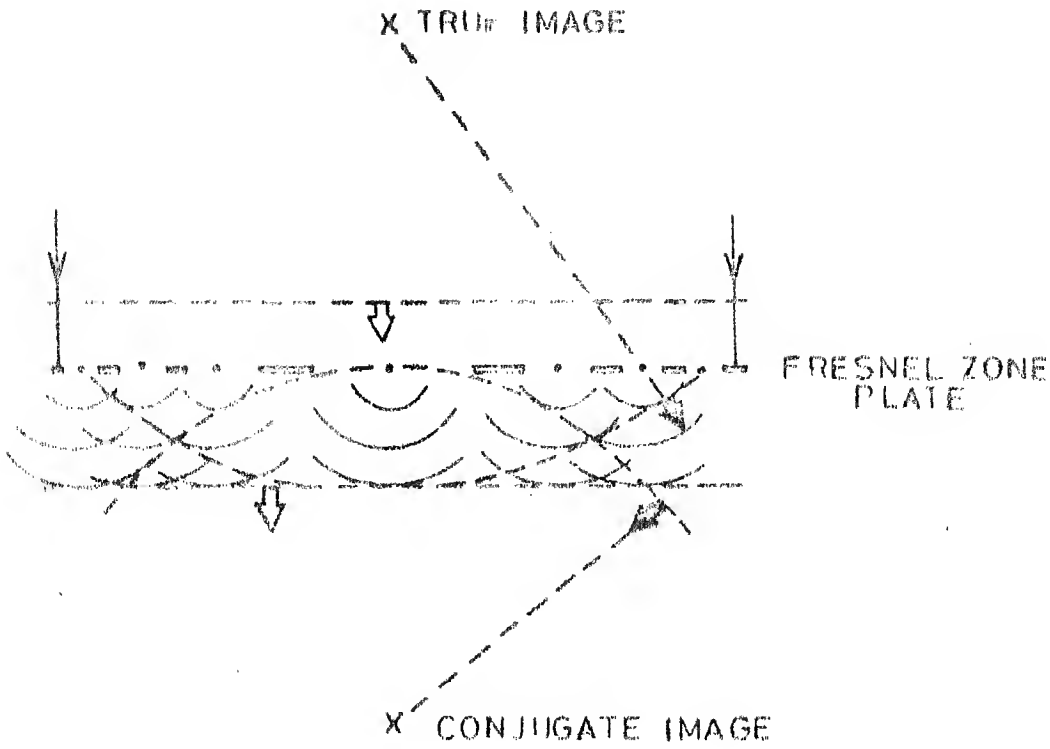

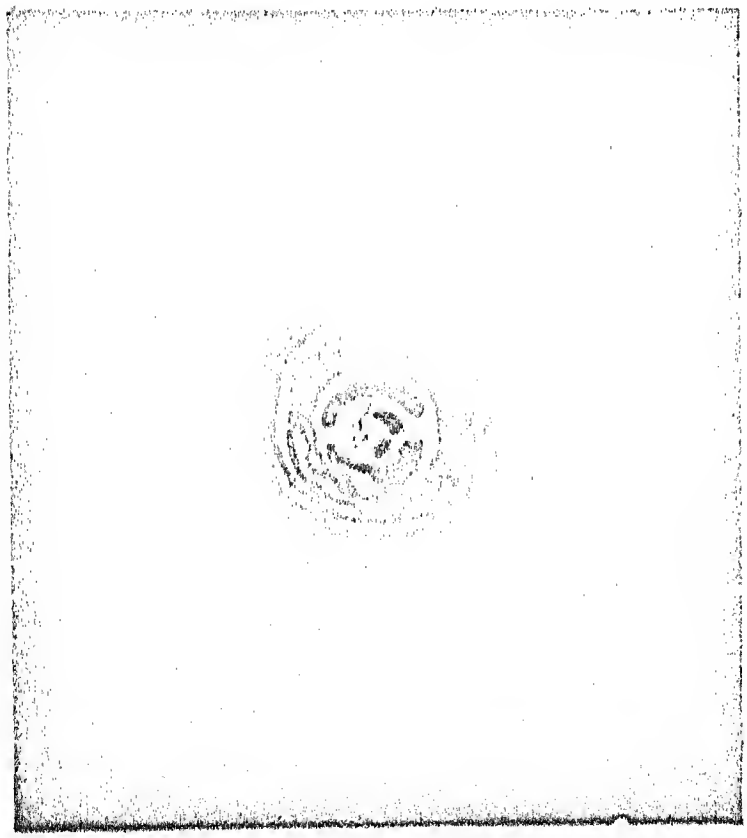

FIG.1·6 HUYGENS' RECONSTRUCTION OF THE FRESNEL ZONE PATTERN

wavefront, again duplicating the beams that caused the original interference pattern. Again we have an extra wave of opposite curvature.

The last example considered was that of an offset Fresnel Zone pattern (Fig.1.4). For completeness we show in Fig. 1.7, the result of introducing this pattern in a beam of light, although one can anticipate the consequences.

The significance of the foregoing discussion is that interferometry has always had the capacity of recording a wavefront and later reconstructing it. These three examples chosen above clearly explain how holography works. The first example (Fig. 1.2) was intended to demonstrate both interference and diffraction. The second example (Fig. 1.3), a slightly more complicated situation, was chosen to show how Gabor Holography works and why it is not successful. Using the Gabor approach, one is reconstructing three beams of light, all occupying the same volume. That is, if one considers Fig. 1.6, one is forced to look at the plane wave and the converging extraneous wave both of which tend to mask the light from the desired wave, when looking for the replica of the spherical wave used in making the interferogram.

The third example, Fig. 1.4, shows how this difficulty is overcome by using an offset in the spherical beam. The same result can be produced by bringing the plane reference wave in at an angle, although in this case the interference

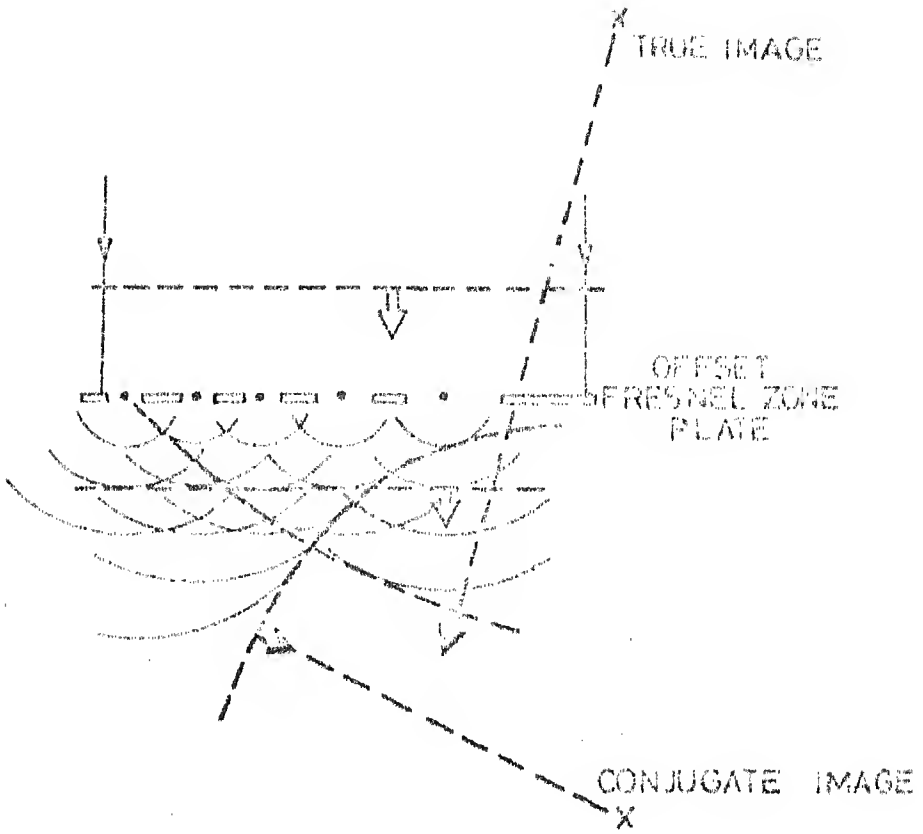

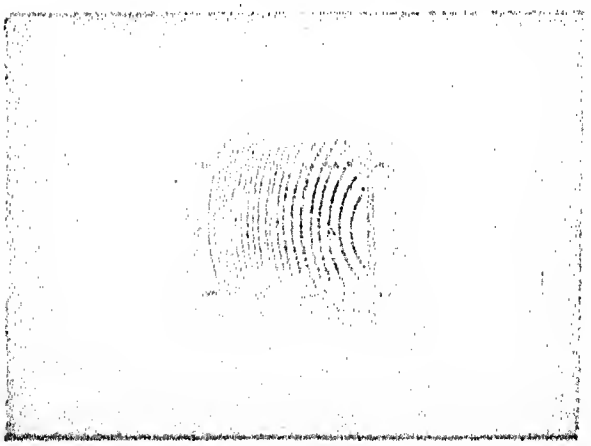

FIG.1·7 HUYGENS' RECONSTRUCTION OF THE OFFSET FRESNEL ZONE PATTERN

pattern is not a circular Fresnel pattern. In this case, all the three diffracted beams are separated in space, thus completely solving the problem of overlap.

To make these discussions conform to what one generally likes to think of as holography, one further step is required, namely, to record and display an image of a complicated object. This step only requires that we accept Huygens' principle which states that any arbitrary wavefront representing the light reflected from a complicated object can be considered to be the sum of a large number of point sources distributed over that wavefront. Since we have shown that we can image a single point or a spherical wave, it is reasonable to suppose that a distribution of points can also be imaged.

The foregoing theory depends upon the overriding principle; that is, that the two beams must be capable of interfering. This, in turn, requires a property of light, known as coherence. A wave is said to be perfectly coherent if its phase structure is fixed with respect to time. The degree of coherence of wave influences the recording of interference fringes and consequently the formation of hologram. In recording a wavefront, the sensitivity or time constant of the detector determines the integration time necessary for recording of interference fringes. If the relative phase of the wave changes during the recording time, the fringes move and quality of the recording is degraded. If the phase of the wavefront fluctuates randomly, the

recording of fringes is best described in terms of the mutual coherence function which is defined as the cross-correlation of the complex functions describing the wave at two points in space at different times under the assumption that waves are all polarized in the same sense and stationary in time. Lasers are commonly thought of as single frequency, highly coherent optical sources. However, they are often multiple frequency sources with relatively low coherence. By proper precautions and controls, a laser with a temporal and spatial coherence properties can be obtained. Sources for Microwave and acoustical wavelengths are normally coherent.

So far we have discussed optical holography but our main interest in this thesis is in some aspects of acoustical holography. First, we will see what are acoustic signals. The term 'Acoustic' applies to all mechanical vibrations and compressional and shear waves having any frequency. A very broad spectral range is encompassed within the field of acoustics. Any mechanical vibration with frequencies ranging from a lower limit of almost 0 Hz to an upper limit of 10^{12} Hz is within the realm of consideration.

Now we will relate the acoustical holography to optical holography. It should be noted that the interference and diffaction are phenomena common to all forms of energy whose propagation can be described in terms of a wave motion. All that is required is the ability to record an interference pattern in the particular type of radiation we happen to be

using and use this pattern to diffract light into a replica of the original wave. In this way it is possible to produce a visual image of an object irradiated with invisible energy.

Photographic film is insensitive to acoustic radiation. Point by point sampling method using one or more acoustical receivers and liquid surface holography are some of the methods developed for recording the acoustic hologram. The recording procedure of these methods is explained in detail in the second chapter.

Thus we have studied the recording of the hologram and reconstruction of the original wave (object wave) on a qualitative physical basis in this Chapter. Chapter 2 deals with the hologram recording and image reconstruction, in mathematical terms. The third chapter discusses the basic principle behind the bispectral passive imaging and the computational aspects involved in estimating the bispectral density. The fourth chapter presents the simulation work that has been done for the reconstruction of images of some idealized objects. The fifth and final chapter discusses the computational results and recommendations for future work. The computer programmes are listed in the Appendix.

CHAPTER 2

CONVENTIONAL HOLOGRAPHY

In Chapter 1, how a modified form of interferometry could be used to record a wavefront was discussed on a qualitative physical basis. This record, in turn could be used to reconstruct the wavefront by the process of diffraction. This method of photography has come to be known as holography after the word 'hologram' coined by Gabor to describe such an interferogram. In this chapter the process is described in mathematical terms.

2.1 Recording Process for Optical Signals

Consider two beams of radiation intersecting on a detecting plane as shown in Fig. 2.1. These two waves come from two transducers driven by the same oscillator. We can describe the optical field at a point (x,y) on the detecting surface due to beam 1 as

$$S_1(x,y) = a_1(x,y)\cos[\omega t + \varphi_1(x,y)] \qquad (2.1)$$

and the field at (x,y) due to beam 2 as

$$S_2(x,y) = a_2(x,y)\cos[\omega t + \varphi_2(x,y)] \qquad (2.2)$$

where a(x,y) is the amplitude of the wave and $\varphi(x,y)$ is the phase of the wave. The total amplitude at (x,y) is the sum of these two individual beams. The result is

$$\begin{aligned} S(x,y) &= S_1(x,y) + S_2(x,y) \\ &= a_1(x,y)\cos[\omega t+\varphi_1(x,y)]+a_2(x,y)\cos[\omega t+\varphi_2(x,y)] \end{aligned} \qquad (2.3)$$

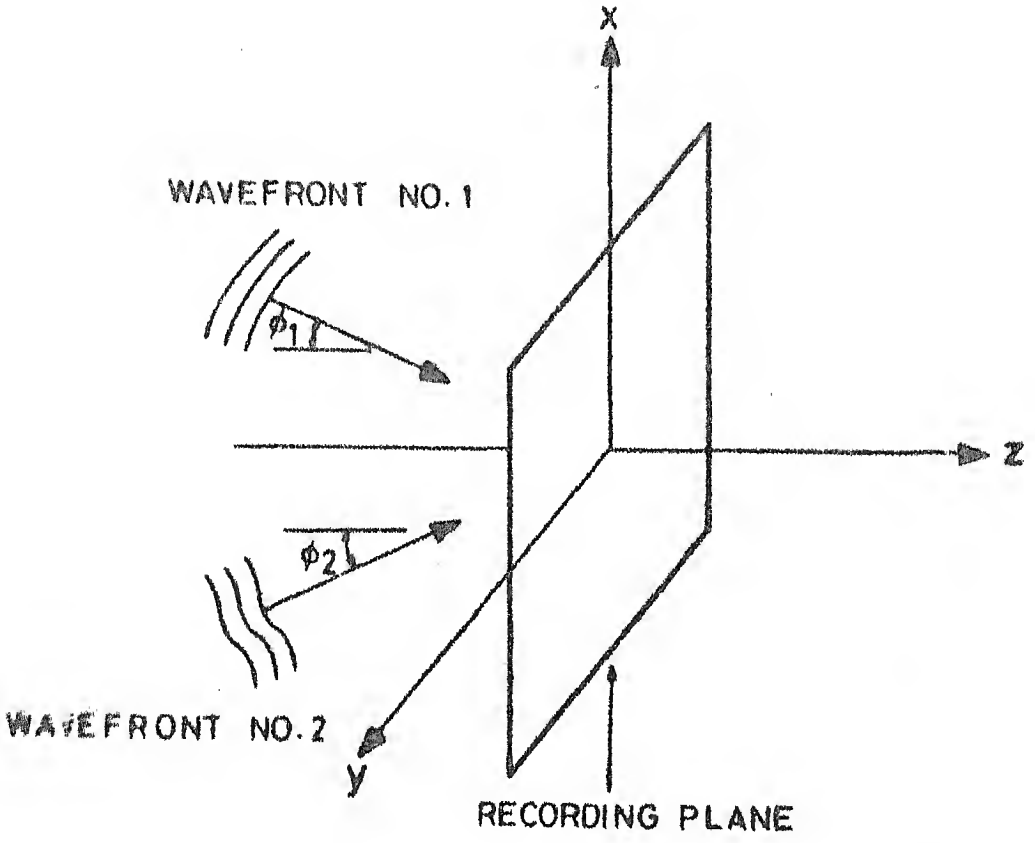

FIG. 2·1 FORMATION OF THE HOLOGRAM

Since no detector exists which can detect the oscillations at optical frequencies, the best that can be done is to measure the intensity. The signal that is actually recorded is therefore some function of intensity, which can be written

$$I(x,y) = \langle [S(x,y)]^2 \rangle_t \tag{2.4}$$

where $\langle \ldots \rangle_t$ denotes a time average over many cycles of radiation.

Substituting eq.(2.3) into eq.(2.4) yields

$$I(x,y) = S_1^2 + S_2^2 + (S_1 S_2)_+ + (S_1 S_2)_-$$

where

$$\begin{aligned} S_1^2 &= \tfrac{1}{2} a_1^2(x,y) \langle [1 + \cos 2(\omega t + \varphi_1(x,y))] \rangle_t \\ S_2^2 &= \tfrac{1}{2} a_2^2(x,y) \langle [1 + \cos 2(\omega t + \varphi_2(x,y))] \rangle_t \\ (S_1 S_2)_+ &= \tfrac{1}{2} a_1(x,y)\, a_2(x,y) \langle \cos(2\omega t + \varphi_1(x,y) \\ &\qquad + \varphi_2(x,y)) \rangle_t \\ (S_1 S_2)_- &= \tfrac{1}{2} a_1(x,y)\, a_2(x,y) \langle \cos(\varphi_1(x,y) - \varphi_2(x,y)) \rangle_t \end{aligned} \tag{2.5}$$

This equation clearly shows why the temporal frequency term is so easily dropped. An oscillating function such as $\cos(\omega t)$ averages to zero, if many cycles are considered. Hence, eq.(2.5) reduces to

$$I(x,y) = \tfrac{1}{2}\{[a_1^2(x,y) + a_2^2(x,y) + a_1(x,y)\, a_2(x,y) \cos(\varphi_1(x,y) - \varphi_2(x,y))]\} \tag{2.6}$$

Note that we have succeeded in preserving phase information even though the recording was done on a phase insensitive medium. This, of course, is the secret of holography.

2.2 Reconstruction Process for Optical Signals

In Chapter 1, it is noted that the wavefront stored on the interferogram could be reconstructed by the process of diffraction of a plane wave. This plane wave can be expressed as

$$S_3(x,y) = a_3(x,y)\cos(\omega t + \varphi_3(x,y)) \qquad (2.7)$$

Suppose we have exposed a photographic plate to the intensity shown in eq.(2.6). After development it possesses a transmittance proportional to the intensity. Then the wave S_3 after passing through the plate is modified by it as

$$\begin{aligned} KI(x,y)\, S_3(x,y) = {} & \frac{K}{2}\left[a_1^2(x,y) + a_2^2(x,y)\right] a_3(x,y)\cos[\omega t+\varphi_3(x,y)] \\ & + \frac{K}{4} a_1(x,y)\, a_2(x,y)\, \{\cos[\omega t+\varphi_1(x,y)-\varphi_2(x,y) \\ & + \varphi_3(x,y)] + \cos[\omega t-\varphi_1(x,y)+\varphi_2(x,y)+\varphi_3(x,y)]\} \end{aligned} \qquad (2.8)$$

where K is a constant.

If we consider the terms one at a time we note that the first term represents the reconstruction wave modified in amplitude. The second term assuming that S_3 is a replica of S_2, becomes

$$\frac{K}{4} a_2^2(x,y)\, a_1(x,y)\cos[\omega t + \varphi_1(x,y)]$$

which we recognise as the original wave, S_1, modified in amplitude. If S_2 happens to be a plane wave, a_2 is a constant and a perfect reconstruction is obtained. With the same reconstruction wave the third term of eq.(2.8) becomes

$$\frac{K}{4} a_2^2(x,y)\, a_1(x,y)\, \cos[\, \omega t - \varphi_1(x,y) + 2\varphi_2(x,y)]$$

This is the extraneous term we referred to earlier. There are several more options available. For example, we could let S_3 be a replica of S_2 with opposite curvature; that is

$$S_3(x,y) = a_2(x,y)\, \cos[\, \omega t - \varphi_2(x,y)]$$

Then the second and third terms of eq.(2.8) become

$$\frac{K}{4} a_2^2(x,y)\, a_1(x,y)\, \cos[\, \omega t + \varphi_1(x,y) - 2\varphi_2(x,y)]$$

and

$$\frac{K}{4} a_2^2(x,y)\, a_1(x,y)\, \cos[\, \omega t - \varphi_1(x,y)]$$

Here we see that the last term becomes a reconstruction of S_1 with opposite curvature and the second term is the extraneous image. Another possible form of S_3 is S_1, giving reconstructed terms.

$$\frac{K}{4} a_1^2(x,y)\, a_2(x,y)\, \cos[\, \omega t + 2\varphi_1(x,y) - \varphi_2(x,y)]$$

and

$$\frac{K}{4} a_1^2(x,y)\, a_2(x,y)\, \cos[\, \omega t + \varphi_2(x,y)]$$

Thus we have reconstructed S_2 and demonstrated the complete ambivalence of the interferometer. While recording the wavefront of one arm we have also recorded the other. Hence either one may be reconstructed by diffracting the other beam through the interferogram. Additionally by using the conjugate of the one of the interfering beams as the diffracting beam we can reconstruct the conjugate of the other.

2.3 Recording of an Acoustic Hologram

In case of acoustic signals, because of their long wavelength, measuring the phase is not a difficult problem. Detectors capable of measuring the amplitude of oscillations of the acoustic signals are readily available. The system used, for recording the hologram is shown in Fig. 2.2. Here the received signal (scanned signal) is multiplied by the oscillator signal (reference signal) and sent through a low pass filter to yield the desired hologram signal. The mathematical procedure is as follows:

$$S_1(x,y) = a_1(x,y)\cos[\omega t + \varphi_1(x,y)] \tag{2.9}$$

After multiplication by $a_2\cos(\omega t + \varphi_2)$, this becomes

$$S'(x,y) = \frac{a_2 a_1(x,y)}{2}\left\{\cos[2\omega t + \varphi_1(x,y) + \varphi_2] + \cos[\varphi_1(x,y) - \varphi_2]\right\} \tag{2.10}$$

After low pass filtering, we are left with

$$S''(x,y) = \frac{a_2 a_1(x,y)}{2}\cos[\varphi_1(x,y) - \varphi_2] \tag{2.11}$$

Comparing eqs.(2.9) and (2.11) we see that we have succeeded in obtaining the same information without the attendant extraneous terms a_1^2 and a_2^2.

The signal $S''(x,y)$ may be stored on a magnetic tape. The only way to get the full amount of information from this data is to reconstruct the wavefront. To do this, the data must be recorded in the form of a hologram. The basic method is to intensity modulate a light source with the stored signal

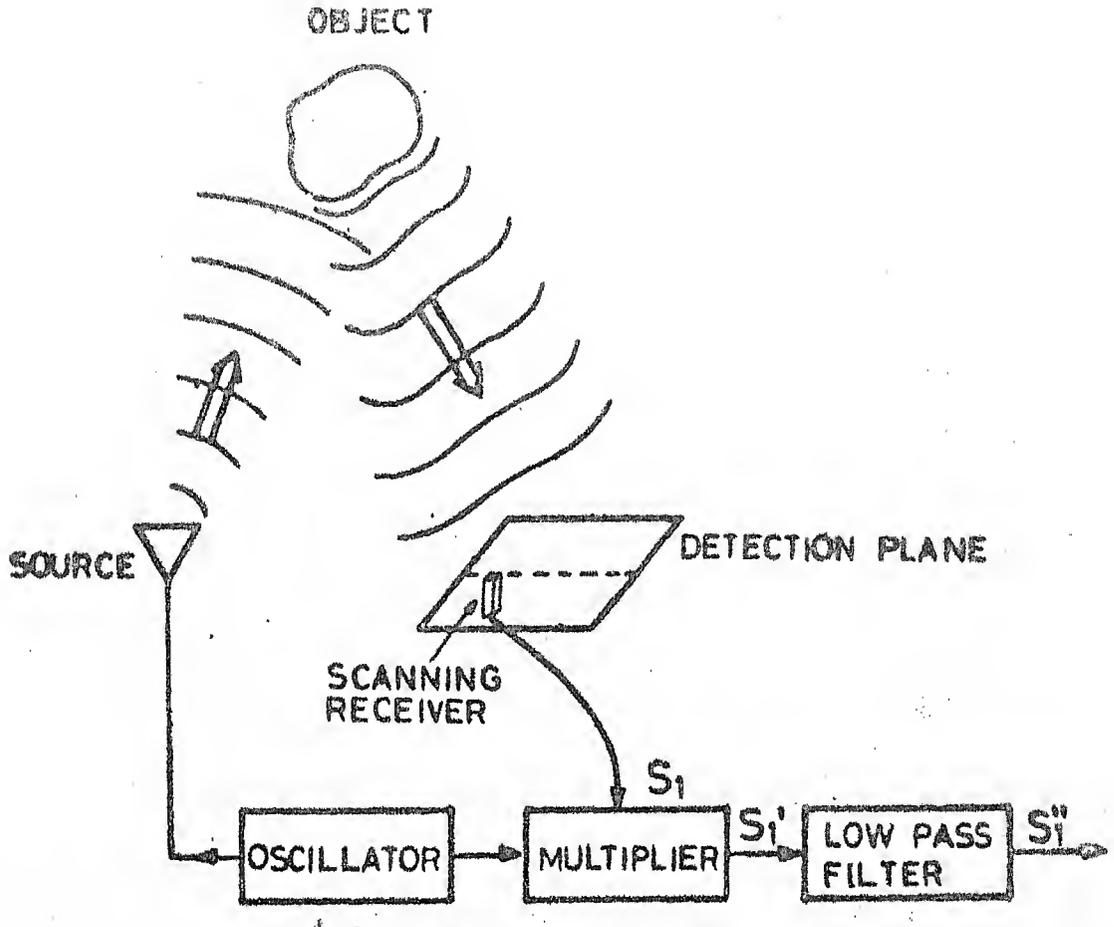

FIG. 2·2 AN ARRANGEMENT USED FOR RECORDING THE ACOUSTICAL HOLOGRAM

on magnetic tape about some average intensity, move it in position and velocity in proportion to that of the detector and record the light on a light-sensitive medium that is shaped proportionately to the surface over which the receiver was scanned.

In practice only planar surfaces have been used, but scan lines in the surfaces have been straight lines or circles. The most common light sources have been an incandescent bulb focussed to a very small point, and the face of a cathode ray tube with a moving intensity modulated spot. The first method requires a mechanical scanning system whereas the second one requires an electronic scanning system. Each method requires a camera to photograph the moving light source. Reconstruction process is same as the one explained for optical signals.

2.4 'Liquid surface holography'

'Liquid surface holography' is another means of recording the interference pattern. The system used for imaging is shown in Fig. 2.3. It includes an object beam transducer that insonifies the object uniformly. The object scatters, diffracts, absorbs energy, and modifies the phase distribution in the wavefront. A pair of acoustic lenses are used to image the sound distribution of the object into the plane of the hologram. The geometry of the wavefront of the reference beam should be simple so that the wavefront can be easily simulated in a beam of light. This means that the wavefront should be either plane or spherical. The object beam and the reference beam should be essentially coherent. The rapid response of the liquid surface

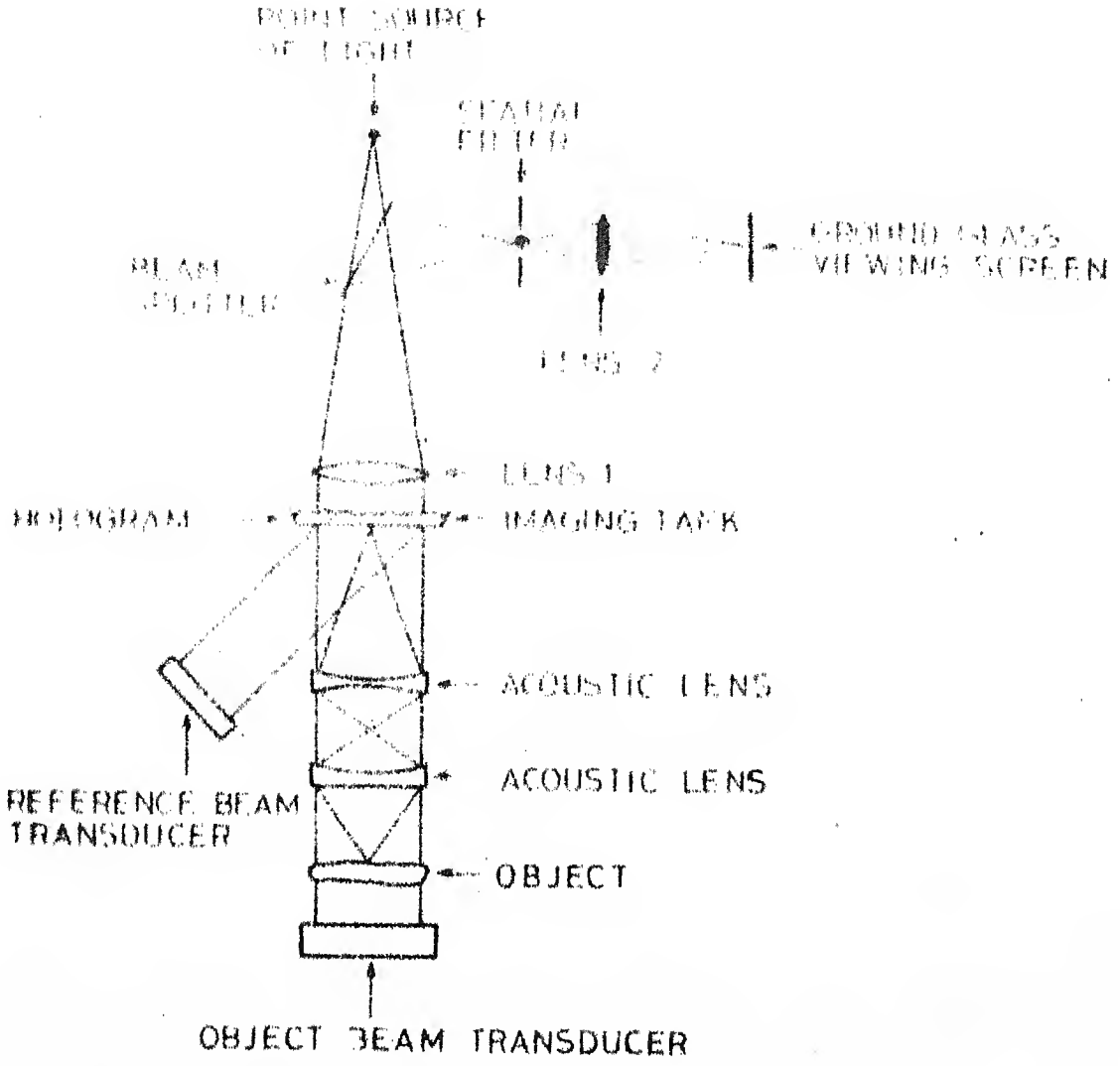

FIG. 2·3 AN ARRANGEMENT FOR IMAGING ULTRA SOUND BY USE OF LIQUID SURFACE ACOUSTICAL HOLOGRAPHY

permits a few percent difference in frequency between the object and the reference beams. The sound field of the object beam mixes with the sound field of the reference beam transducer to form an interference pattern at liquid-air interface in the imaging tank. The interference pattern is imprinted in the liquid surface as variations in elevation.

An imaging tank is used to isolate the hologram from liquid surface disturbances in the main (object) tank. Use of a imaging tank also allows the use of different liquids for hologram formation and for object immersion. Thus, liquids can be chosen which are optimum for each of these purposes.

The hologram surface imposes phase variations in the reflected beam of light which cause diffraction of the light. First order diffracted light is passed at the spatial filter which blocks all other light reflected from the hologram surface.

Lens 1 is used to image the point source of light at the plane of the spatial filter after reflection from hologram surface. Lens 2 images the hologram surface on the ground glass viewing screen. Since the hologram is a focussed image type, the ground glass screen displays the desired image of the object. Although the hologram modifies only the phase of the light, there is amplitude imaging because the amount of light diffracted into the first order varies as the amplitude of the interference pattern on the liquid surface, which inturn, varies as the amplitude of the wave in the object beam.

2.5 Recording of the Hologram Employing Digital Signal Processing Methods

An alternative solution for the reconstruction of the wavefront of the object wave is using digital signal processing methods. Here, we use two receivers; one is fixed and the other scans over a hologram plane.

The signal detected by the scanning receiver can be expressed as

$$S_1(t,x,y) = A(x,y) \cos[\, \omega t + \varphi_1(x,y)] + n_1(t)$$

where (x,y) is a point on the hologram plane and $n_1(t)$ is the additive Gaussian noise. $A(x,y)$ and $\varphi(x,y)$ are amplitude and phase distributions of the scanned signal.

The signal detected by the fixed receiver

$$S_2(t) = \text{reference signal} = B \cos(\, \omega t + \varphi_2) + n_2(t)$$

where $n_2(t)$ is additive Gaussian noise. Both $n_1(t)$ and $n_2(t)$ are assumed to be independent of the received signals, but not so in between them.

The cross-power spectral density between the object and reference waves is computed at all the scanned points on the hologram plane and is given by the following expression:

$$C_{S_1S_2}(\, \omega\, , x,y) = A(x,y)\, B \cos(\varphi_1(x,y) - \varphi_2) + C_{n_1n_2}(\omega)$$

where $C_{n_1n_2}$ is cross-power spectral density between the noises $n_1(t)$ and $n_2(t)$.

It is clear from the above expression that the cross-power spectral density $C_{s_1s_2}$ contains the amplitude and phase

information of the object wave. Hence the cross-power spectral density computed at each point on the hologram plane forms the hologram signal in the Fourier domain. The image is retrieved as a computer print-out, simply by performing an inverse Fourier transform on the hologram signal.

The signal processing carried out in the computer is shown in Fig. 2.4.

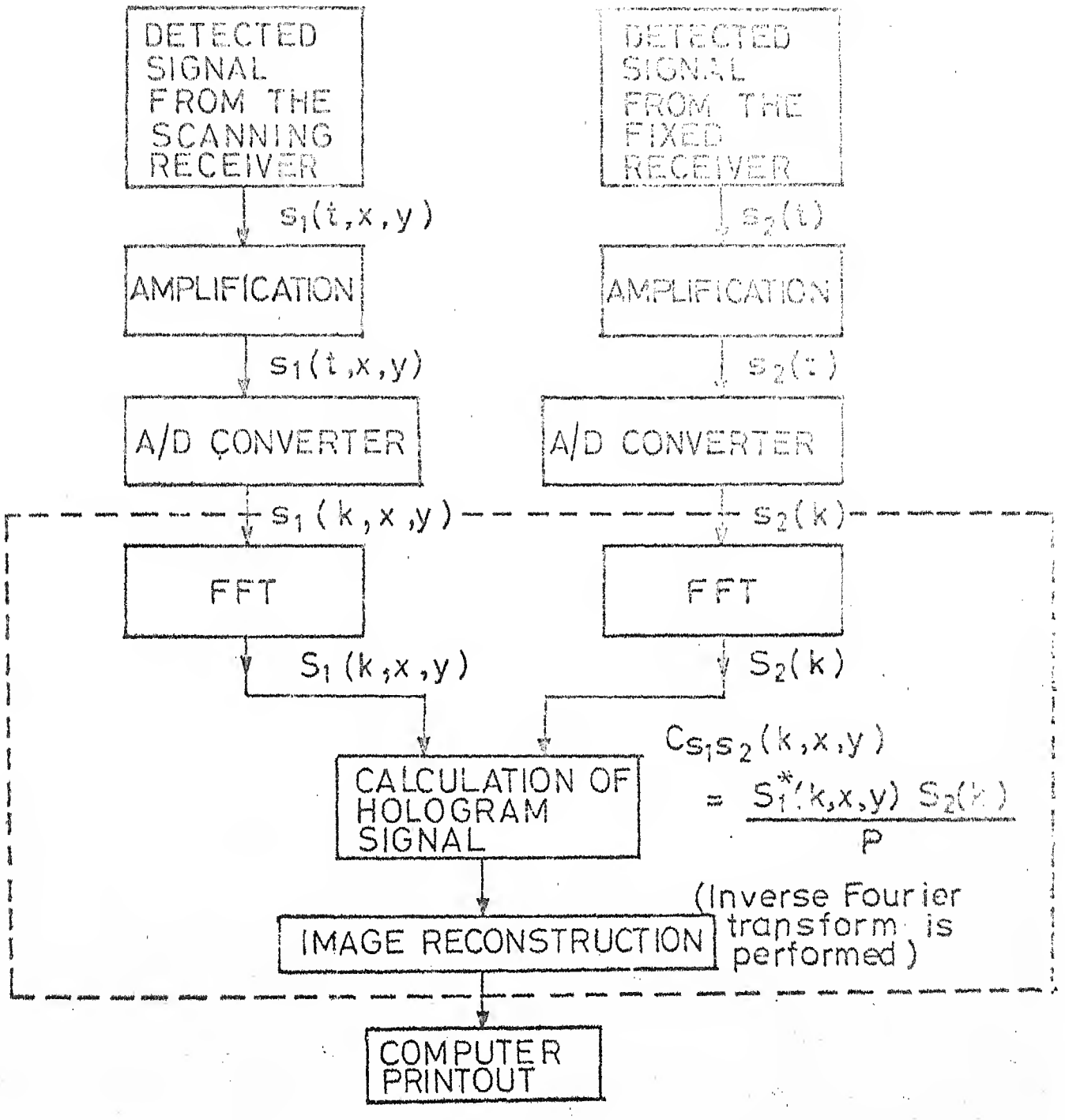

FIG.2.4 SIGNAL PROCESSING STEPS IN CONVENTIONAL DIGITAL HOLOGRAPHY

CHAPTER 3

BISPECTRAL HOLOGRAPHY

The amplitude and phase of the object wave can be obtained by cross correlating the object wave and reference wave on the hologram plane. This is the conventional way of recording the hologram, which was discussed in the last chapter. If the signals illuminating the object or object emitted signals are non-Gaussian the phase of the signals can be derived from bispectra or higher order spectral analysis. The condition that signal should be non-Gaussian is satisfied in many practical applications, since any periodic signal can be regarded as a non-Gaussian signal and self-emitting signals from objects such as complicated mechanical systems can also be considered as non-Gaussian signals.

Two receivers one fixed and the other scanning over the hologram plane are used to obtain the holographic information. Auto-bispectral and cross-bispectral analysis are carried out on the detected signals. By taking their ratio the required information is obtained. This is explained in the later parts of this chapter. Image reconstruction is performed by using conventional holographic methods.

Bispectral analysis provides a means of obtaining holograms free from additive Gaussian noises in the amplitude and shape of the power spectra.

The application of bispectral analysis is equivalent to the utilization of mutual relations among three frequency components, that satisfy $f_1+f_2+f_3 = 0$. In the case of a Gaussian signal each frequency component is independent. These facts produce very effective and special features when this method is applied to holographic imaging systems.

The principle of bispectral analysis for getting the hologram signal is dealt with in the following sequence. First the descrpition of the data acquisition system and assumptions postulated for generalized object illuminating signals and additive noise are given. Secondly by discussing the properties of the bispectra of the signals detected at the hologram plane, the procedure required to obtain the hologram signal is derived. Finally the image reconstruction process is discussed briefly.

3.1 Theory of Bispectral Imaging[2]

Consider the system shown in Fig.3.1, where non-Gaussian random signals $S_i(p,t)$ $(i = 1,...M)$ are assumed to be emitted from the object plane π_1. $n(t)$ is the noise added in the channel. These signals are received at the hologram plane π_2 by two receivers. One is a fixed receiver R_1, which is assumed to be located at the origin and the other one is scanning receiver R_2, located at r_2 on the same plane. $n_1(t)$ and $n_2(t)$ are the noises added to the detected signals at receivers R_1 and R_2 respectively. The signals on the

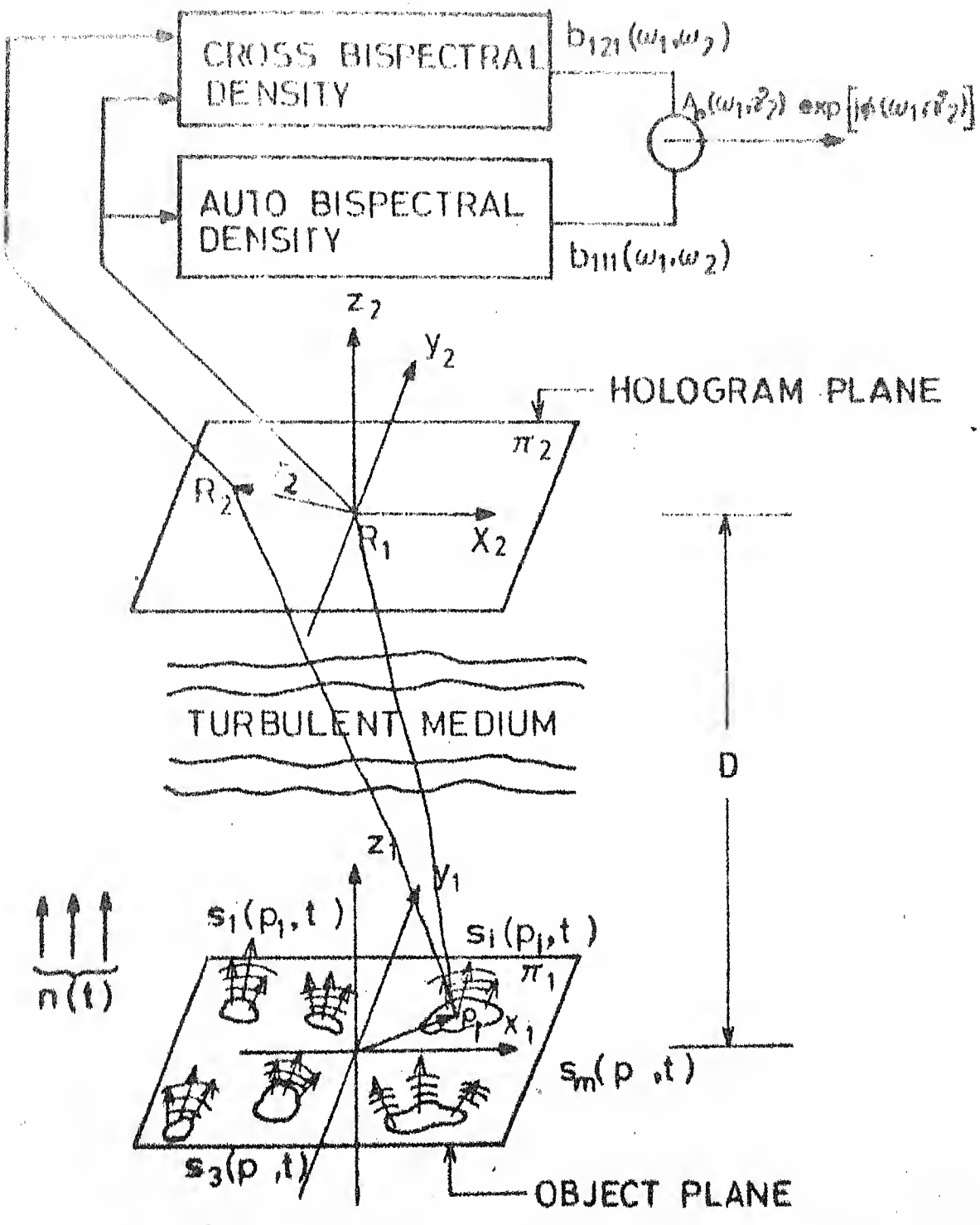

FIG. 3·1 SCHEMATIC CONSTRUCTION AND SIGNAL PROCESSING OF BISPECTRAL HOLOGRAPHY

plane π_2 may be considered as sum of the following three components.

a) Signals from the object plane.

b) Surrounding noises $n_s(t)$, $n(t)$.

c) The additive noises $n_1(t)$, $n_2(t)$ which are added at the corresponding receivers.

Information about the amplitude and phase of the wavefront of a given frequency at each point on the hologram plane is required to construct the hologram.

Assumptions: The assumptions postulated for the object illuminating signals and the transmission medium are given below:

i) The object illuminating signals $S_i(p,t)$ $(i=1,\ldots M)$ are harmonizable (this means that $S_i(p,t)$ can be expressed as the first expression of Eq.(3.1)) and third order weakly stationary non-Gaussian signals and without loss of generality they are assumed to have zero mean.

$$S_i(p,t) = \int_{-\infty}^{\infty} \exp(j\omega t)\, dZ_i(\omega)$$

$$\langle dZ_i(\omega) \rangle = 0 \qquad (3.1)$$

$$b_i(\omega_1, \omega_2)d^2\omega = \langle dZ_i(\omega_1)\, dZ_i(\omega_2)\, dZ_i(\omega_3) \rangle_{\omega_1+\omega_2+\omega_3=0}$$

where $\langle . \rangle$ denotes an ensemble averaging operation and $b_i(\omega_1, \omega_2)$ represents the bispectral density of $S_i(p,t)$.

ii) Noises are assumed to be Gaussian. No restriction is made about their power spectra. It is also assumed that they are statistically independent of the object illuminating signals $S_i(t)$ $(i = 1,\ldots M)$. No assumption is made about the independence among these noises.

The received signals $u_q(r_q,t)$ $(q = 1,2)$ at the two receivers can be expressed as follows:

$$u_q(r_q,t) = \int_{\pi_1}\int_{-\infty}^{\infty} \sum_{i=1}^{M} A_i(p)Z_i(\omega)H(\omega;\ p,r_q)\ e^{j\omega t}\ d\omega\ dp + n(t) + n_q(r_q,t)\ ,\quad q=1,2 \qquad (3.2)$$

where $A(p)$ is the amplitude of the object wave at a point p on the object plane and $H(\omega;\ p,\ r)$ is given by

$$\int_{\infty}^{\infty} h(\tau,\ p,\ r)e^{-j\omega\tau}\ d\tau$$

where τ is the time instant at which you apply the input and r is an observation point on the hologram plane.

Under the assumption that turbulences of the medium affect only as random phase shifters on propagating waves and their variation in time are so slow that they can be regarded as fixed values while bispectral analysis for each data is carried out, the transfer function $H(\omega;\ p,r)$ is expressed as follows:

$$H(\omega;\ p,\ r) = \frac{G(\omega)}{j\lambda\, d(p,r)} \exp[-jkd(p,r)]\exp[ja(\omega;\ p,r)] \qquad (3.3)$$

where λ, k denote respectively, the wavelength and wave-number of a wave with angular frequency ω; $a(\omega; p,r)$ is the accumulated phase shift due to random medium between p and r; $G(\omega)$ is the amplitude transmitting factor.

Another assumption made on channel is the accumulated phase shifts caused by random medium are subjected to the same probability distribution for any p and r, so that they are expressed as a random variable with index ω as $b(\omega)$.

The transfer function of the medium described above does not take the multipath effect into consideration. The reason for this is that the size of the random scatterers is much greater than a wavelength. Because of that the wave scattered by the particle is largely confined to a small angle in the forward direction.

Substituting $H(\omega; p,r)$ in Eq.(3.2), we get

$$u_q(r_q,t) = \sum_{i=1}^{M} \int_{\infty}^{\infty} \left[\int_{\pi_1} \frac{G(\omega)}{j\lambda d(p,r_q)} A_i(p) \exp[-jkd(p,r_q)] \right.$$

$$\left. \exp[ja(\omega;p,r_q)]dp \right] \exp(j\omega t)dZ_i(\omega)+N_q(r_q,t)$$

$$q = 1,2 \qquad (3.3)$$

where $N_q(r_q,t)$ $(q = 1,2)$ are the overall corrupting noises at the receivers and they are independent of $S_i(p,t)$ $(i = 1, \ldots M)$ from the assumption (ii). $A(p)$ is the amplitude of the emitting signal at a point p on the object plane.

Consider the signals $X_i(t) = X(t) + Y_i(t)$ $(i = 1,2)$ where $Y_i(t)$ $(i = 1,2)$ are weakly-stationary Gaussian signals

and $X(t)$ is a third order stationary non-Gaussian signal and independent of $Y_i(t)$ $(i = 1,2)$. Then the third order cross-correlation function $R_{X_1X_2X_1}(\tau_1,\tau_2)$ between $X_1(t)$ and $X_2(t)$ is given as follows:

$$R_{X_1X_2X_1}(\tau_1,\tau_2) = \langle [X_1(t) - \langle X_1(t) \rangle][X_2(t+\tau_1) - \langle X_2(t+\tau_1) \rangle]$$

$$[X_1(t+\tau_2) - \langle X_1(t+\tau_2) \rangle] \rangle$$

$$= R_{XXX}(\tau_1,\tau_2) + R_{Y_1Y_2Y_1}(\tau_1,\tau_2)$$

$$= R_{XXX}(\tau_1,\tau_2)$$

where the fact that the third order correlation function of any Gaussian signal is identically zero is used.

By applying this relation to $u_q(r_q,t)$ $(q = 1,2)$ in Eq.(3.3), the third order cross-correlation function $R_{u_1u_2u_3}(\tau_1,\tau_2)$ which is abbreviated as $R_{121}(\tau_1,\tau_2)$ can be derived as

$$R_{121}(\tau_1,\tau_2) = \sum_{i_1=1}^{M} \sum_{i_2=1}^{M} \sum_{i_3=1}^{M} \int_{-\infty}^{\infty} d\omega_1 \int_{-\infty}^{\infty} d\omega_2 \; b_{S:i_1i_2i_3}(\omega_1,\omega_2)$$

$$\frac{G(\omega_1)\, G(\omega_2)\, G(-\omega_1-\omega_2)}{-j^3 \lambda_1 \lambda_2 (\lambda_1^{-1} + \lambda_2^{-1})^{-1}} \exp[j(\tau_1\omega_1+\tau_2\omega_2)]$$

$$\left\langle \exp\left\{ j[b(\omega_1)+b(\omega_2)+b(-\omega_1-\omega_2)] \right\} \right\rangle$$

$$\int_{\pi_1} \frac{A_{i_1}(p_1)}{d_1'} \exp(-jk_1d_1')dp_1 \int_{\pi_1} \frac{A_{i_2}(p_2)}{d_2} \exp(-jk_2d_2)d$$

$$\int_{\pi_1} \frac{A_{i_3}(p_3)}{d_3} \exp(j(k_1+k_2)d_3)dp_3 \qquad (3.4)$$

where $d_1' = d(p_1,r_2)$ and $d_i = d(p_i,r_i)(i=2,3)$

Then the cross-bispectral density $B_{121}(\omega_1, \omega_2)$, which is defined as the Fourier transform of $R_{121}(\tau_1, \tau_2)$, can be expressed as

$$(1/2\pi)^2 \sum_{i_1=1}^{M} \sum_{i_2=1}^{M} \sum_{i_3=1}^{M} b_{S:i_1 i_2 i_1}(\omega_1, \omega_2) \frac{G(\omega_1)G(\omega_2)G(-\omega_1-\omega_2)}{-j^3\lambda_1\lambda_2(\lambda_1^{-1}+\lambda_2^{-1})^{-1}}$$

$$< \exp\{j[b(\omega_1) + b(\omega_2) + b(-\omega_1 - \omega_2)]\} > \int_{\pi_1} \frac{A_{i_1}(p_1)}{d_1'} \exp(-jk_1 d_1')dp_1$$

$$\int_{\pi_1} \frac{A_{i_2}(p_2)}{d_2} \exp(-jk_2 d_2)dp_2 \int_{\pi_1} \frac{A_{i_3}(p_3)}{d_3} \exp(j(k_1+k_2)d_3)dp_3 \tag{3.5}$$

In the same way, the auto-bispectral density $B_{111}(\omega_1, \omega_2)$ is obtained from Eq.(3.5) and is given below:

$$B_{111}(\omega_1, \omega_2)$$

$$= (1/2\pi)^2 \sum_{i_1=1}^{M} \sum_{i_2=1}^{M} \sum_{i_3=1}^{M} b_{S:i_1 i_2 i_1}(\omega_1, \omega_2) \frac{G(\omega_1)G(\omega_2)G(-\omega_1-\omega_2)}{-j^3\lambda_1\lambda_2(\lambda_1^{-1}+\lambda_2^{-1})^{-1}}$$

$$< \exp\{j[b(\omega_1)+b(\omega_2)+b(-\omega_1-\omega_2)]\} > \int_{\pi_1} \frac{A_{i_1}(p_1)}{d_1} \exp(-jk_1 d_1)dp_1$$

$$\int_{\pi_1} \frac{A_{i_2}(p_2)}{d_2} \exp(-jk_2 d_2)dp_2 \int_{\pi_1} \frac{A_{i_3}(p_3)}{d_3} \exp(j(k_1+k_2)d_3]dp_3 \tag{3.6}$$

Equations (3.5) and (3.6) give the bispectra of the signals at the hologram plane and they are expressed as the product of the following three main terms: (i) the term which depends on the bispectrum of the object illuminating signals $S_i(p,t)$ $(i = 1,\ldots M)$, (ii) the term due to the phase turbulence at three angular frequency components $\omega_1, \omega_2, \omega_3$

where $\omega_1 + \omega_2 + \omega_3 = 0$; and (iii) the object dependent term. In the expressions (3.5) and (3.6) the difference is only the use of d_1' or d_1; thus if the ratio between them is taken, the other factors get cancelled.

Derivation of Hologram Signal from Bispectral Analysis: The data required for hologram signals are the relative amplitude and phase of the object waves at the hologram plane. They may be expressed as follows:

$$A_o(\omega;r)\exp[j\varphi_o(\omega;r)] = \frac{A_s(\omega;r)\exp[j\varphi_s(\omega;r)]}{A_r(\omega;r)\exp[j\varphi_r(\omega;r)]}$$

$$= \frac{A_s(\omega;r)}{A_r(\omega;r)}\exp\, j[\varphi_s(\omega;r) - \varphi_r(\omega;r)] \qquad (3.7)$$

where $A_r \exp(j\varphi_r)$ is a reference wave and $A_s \exp(j\varphi_s)$ is the object wave at an observing or scanning point r on the plane. Eqs.(3.5) and (3.6) show that the hologram signal at a scanning point r_2 can be immediately given by the following ratio:

$$\frac{B_{u:12l}(\omega_1,\omega_2)}{B_{u:111}(\omega_1,\omega_2)} = \frac{\sum_{i_1=1}^{M}\int_{\pi_1}\frac{A_{i_1}(p_1)}{d_1'}\exp(-jk_1d_1')dp_1}{\sum_{i_1=1}^{M}\int_{\pi_1}\frac{A_{i_1}(p_1)}{d_1}\exp(-jk_1d_1)dp_1}$$

$$= \hat{A}_o(\omega_1;\, r_2)\exp[i\hat{\varphi}_o(\omega_1;\, r_2)] \qquad (3.8)$$

where $B_{u:111}(\omega_1,\omega_2)$ is assumed to be non-zero.

Equation (3.8) implies that the hologram signal can be obtained as the ratio of the cross-bispectrum and auto-bispectrum of signals at two points on the hologram plane. In this expression, only the desired factors are obtained and the terms which depend on the bispectrum of the signal and the turbulences are cancelled because the ratio is used. Equation (3.8) also indicates that the result is free from additive Gaussian noises.

Image is reconstructed by carrying out the following operation:

$$|I(p')| = \left| \int_{\pi_2} \frac{\hat{A}_o(\omega_1; r)}{j\lambda_2 d(r,p')} \exp[j\hat{\varphi}_o(\omega_1;r)] \exp[jk_2 d(r,p')]dr \right|$$

where p' denotes an image point to be reconstructd and d(r,p') denotes the distance between r and p'.

3.2 The Computational Procedure Involved in Estimating the Bispectral Density

The signals detected by the scanning receiver and fixed receivers are $x_1(t)$ (object signal) and $x_2(t)$ (reference signal)respectively. Their third order correlation functions of $x_1(t)$ and $x_2(t)$ are assumed to be ergodic.

Then the third order auto-correlation function $x_q(t)$ $(q = 1,2)$ is defined as

$$R_{111}(\tau_1,\tau_2) = \lim_{T\to\infty} \frac{1}{T} \int_0^T x_q(t)x_q(t+\tau_1)x_q(t+\tau_2)\, dt \qquad q = 1,2$$

Hence observing the signal $x_q(t)$ $(q = 1,2)$ over a period T,

one can compute

$$R_{111T}(\tau_1,\tau_2) = \frac{1}{T}\int_0^T x_q(t)\, x_q(t+\tau_1)\, x_q(t+\tau_2)\, dt \qquad q = 1,2$$

To compute $R_{111}(\tau_1,\tau_2)$, one has to observe the signal over many such intervals of time period T, and has to compute $R_{111T}(\tau_1,\tau_2)$ each time. Then the average of such $R_{111T}(\tau_1,\tau_2)$'s gives an estimate of $R_{111}(\tau_1,\tau_2)$, whose Fourier transform is nothing but an estimate of the auto-bispectral density of x(t). An alternate way of doing this is to compute $B_{111T}(\omega_1, \omega_2)$ (Fourier transform of $R_{111T}(\tau_1,\tau_2)$) each time after observing the signal over a period T and then taking averages of such $B_{111T}(\omega_1, \omega_2)$'s. First we will see what is $B_{111T}(\omega_1, \omega_2)$ in terms of $X(\omega)$.

$B_{111T}(\omega_1, \omega_2)$ is defined as $F(R_{111T}(\tau_1, \tau_2))$ where $F(\ .\ )$ denotes the Fourier transform. Therefore,

$$B_{111T}(\omega_1, \omega_2) = \frac{1}{T}\int_0^T\int_{-\infty}^{\infty}\int_{-\infty}^{\infty} x(t)x(t+\tau_1)x(t+\tau_2)e^{-j\omega_1\tau_1}e^{-j\omega_2\tau_2}\, dt\, d\tau_1\, d\tau_2$$

$$= \frac{1}{T}\int_0^T\int_{-\infty}^{\infty}\int_{-\infty}^{\infty} x(t)x(\tau_1)e^{j\omega t}\, x(\tau_2)e^{-j\omega_2 t}\, e^{-j\omega_1\tau_1}\, e^{-j\omega_2\tau_2}\, dt\, d\tau_1\, d\tau_2$$

$$= \frac{1}{T}\int_{-\infty}^{\infty} x(\tau_1)e^{-j\omega_1\tau_1}\, d\tau_1 \int_{-\infty}^{\infty} x(\tau_2)e^{-j\omega_2\tau_2}\, d\tau_2 \int_0^T x(t)\, e^{j(\omega_1+\omega_2)t}\, dt$$

[since x(t) is observed only for an interval T, outside this interval its value is zero. Hence we can take the limits from $-\infty$ to $+\infty$]

$$= \frac{1}{T}\, x(\omega_1)x(\omega_2)x^*(\omega_1+\omega_2)$$

The cross-bispectral density of $x_1(t)$ and $x_2(t)$ is defined as

$$B_{121}(\omega_1, \omega_2) = F(R_{121}(\tau_1, \tau_2))$$

To get an estimate of $B_{121}(\omega_1, \omega_2)$, the same procedure that is discussed above for estimating $B_{111}(\omega_1, \omega_2)$ is adapted here. Before actually going to the discussion of the computational procedure involved we will express $B_{121T}(\omega_1, \omega_2)$ in terms of $x_1(\omega)$ and $x_2(\omega)$.

$B_{121T}(\omega_1, \omega_2)$ is defined as $F(R_{121T}(\tau_1, \tau_2))$.

$$B_{121T}(\omega_1,\omega_2) = \frac{1}{T} \int_0^T \int_{-\infty}^{\infty} \int_{-\infty}^{\infty} x_1(t)x_2(t+\tau_1)x_1(t+\tau_2)e^{-j\omega_1\tau_1} e^{-j\omega_2\tau_2} \, dt \, d\tau_1 \, d\tau_2$$

$$= \frac{1}{T} \int_0^T x_1(t) \int_{-\infty}^{\infty} x_2(t+\tau_1)e^{-j\omega_1\tau_1} \, d\tau_1 \int_{-\infty}^{\infty} x_1(t+\tau_2)e^{-j\omega_2\tau_2} \, d\tau_2$$

$$= \frac{1}{T} \int_0^T x_1(t) \int_{-\infty}^{\infty} x_2(\tau_1) \, e^{j\omega t} \, e^{-j\omega_1\tau_1} \, d\tau_1$$

$$\int_{-\infty}^{\infty} x_1(\tau_2) \, e^{j\omega_2 t} \, e^{-j\omega_2\tau_2} \, d\tau_2$$

$$= \frac{1}{T} \int_{-\infty}^{\infty} x_1(t)e^{j(\omega_1+\omega_2)t} \int_{-\infty}^{\infty} x_2(\tau_1)e^{-j\omega_1\tau_1} \, d\tau_1$$

$$\int_{-\infty}^{\infty} x_1(\tau_2)e^{-j\omega_2\tau_2} \, d\tau_2$$

$$= \frac{1}{T} x_2(\omega_1) \, x_1(\omega_2) \, x_1^*(\omega_1+\omega_2) \qquad (3.23)$$

Thus the expressions for $B_{111T}(\omega_1,\omega_2)$, $B_{121T}(\omega_1,\omega_2)$ are derived, which are the triple products of the Fourier coefficients of $x_q(t)$ $(q = 1,2)$. Hence to get good estimates of $B_{111}(\omega_1,\omega_2)$ and $B_{121}(\omega_1,\omega_2)$ one has to average over many such triple products.

The computations may be surprisingly expensive despite the FFT. Moreover, all the pitfalls known from ordinary power spectrum analysis occur here too, some of them with new twists. Thus it seems worthwhile to describe and evaluate the different procedures in detail.

Assume that the bispectrum is to be estimated for frequencies between 0 and $\omega_0/2$ with a bandwidth Δ_0. Hence a sampling rate of ω_0 samples per unit time is atleast needed and uninterrupted records whose size is atleast $N_0 = \omega_0/\Delta_0$. Prefiltering of the frequencies above $\omega_0/2$ is necessary to avoid aliasing. A total of K records (not necessarily consecutive), each of length $N = MN_0$ is assumed to be available. The value of N should be convenient for the FFT, say a power of 2 and M preferably is an odd integer ($M = 2L+1$). To satisfy both conditions a compromising value of N_0 may have to be chosen. Also, it may be necessary to adjust the records, either by adding zeroes at the ends or by allowing some overlap between consecutive records, to reach the exact length N; the final results will have to be corrected for these adjustments. The total number of points is of the order $N_{tot} = KN$.

Because of its symmetry, it suffices to estimate the bispectral density $B(\omega_1, \omega_2)$ in the triangle determined by the equalities.

$$0 \leq \omega_2 \leq \omega_1 , \quad \omega_1 + \omega_2 \leq \omega_0/2.$$

Number the records j = 1,2,...K. For each of them the following operations are performed:

1) Subtract the average and remove a linear trend if necessary.

2) Adding zeroes if necessary to obtain a convenient length N for the FFT.

Numbering the observations in the thus modified sample from 0 to N-1 : $x_o\ x_1 \cdots x_{n-1}$.

3) Fast Fourier transform is performed which gives the Fourier coefficients

$$X(\omega_k) = \sum_{i=o}^{N-1} x_i \exp(-j2\pi i\ k/N) \quad 0 \le k \le N/2$$

4) Estimate the bispectral density $B(\omega_1, \omega_2)$ at $(\omega_k, \omega_L) = (\frac{k\ \omega_o}{N}, \frac{L\omega_o}{N})$ where k,L = 0,1...N/2.

a) Over a quadratic window

$$\hat{B}_j(\omega_1,\omega_2)\ \Delta_o^2 = \sum_{k_1=-L}^{L} \sum_{k_2=-L}^{L} X(\omega_1+k_1)X(\omega_2+k_2)X^*(\omega_1+\omega_2+k_1+k_2)$$

or more symmetrically,

b) over a hexagonal window

$$\hat{B}(\omega_1,\omega_2)\ \Delta_o^2 = \frac{4M^2}{3M^2+1} \sum_{k_1=-L}^{L} \sum_{k_2=-L}^{L} X(\omega_1+k_1)X(\omega_2+k_2)$$

$$X^*(\omega_1+\omega_2+k_1+k_2)$$

where the sum is extended over all k_1, k_2 satisfying

$$|k_1| \le L\ ,\ |k_2| \le L,\ |k_1+k_2| \le L$$

5) Finally, average over k pieces

$$\hat{B}(\omega_1, \omega_2) = \frac{1}{k} \sum_{j=1}^{k} B_j(\omega_1, \omega_2)$$

Part 4 is most expensive term in terms of computer time.

Procedure A: (Average in the Frequency domain): Evaluate operation 5 in the straightforward fashion, e.g. in case (a)

$$\hat{B}_j(\omega_1,\omega_2) \quad \Delta_o^2 = \sum_{k_1=-L}^{L} X(\omega_1+k_1) \sum_{k_2=-L}^{L} X(\omega_2+k_2)$$

$$X^*(\omega_1+\omega_2 + k_1 + k_2)$$

Procedure B: (Complex demodulation)

(1) Put $X^{\omega_L}(\omega_k) = X(\omega_L + \omega_k)$ for $|k| \leq L$

$= 0$ otherwise

$$X^{\omega_L}(\omega_k) = X(\omega_k + \omega_L) \quad \text{for} \quad |K| \leq 2L$$

$= 0$ otherwise.

This means that we apply a narrow band pass filter and shift frequencies to zero.

(2) Transform back-into the time domain. Let $n \geq 2M$ be the least number admitting an efficient FFT. Interpret index k modulo n and compute the finite Fourier transforms.

$$X^{\omega_L}(s) = \sum_{K} X^{\omega_L}(\omega_k) \exp(2\pi isk/N)$$

and similarly for $X^{\omega_L}(\omega_k)$, giving $x^{\omega_L}(s)$.

3) Average in the time domain: In case (a) compute

$$\hat{B}_j(\omega_k, \omega_L)\ \Delta_o^2 = \frac{1}{n} \sum_{s=o}^{n-1} x^{\omega_k}(s)\ x^{\omega_L}(s)\ \tilde{x}^{(\omega_k+\omega_L)}(s)$$

In case (b) compute

$$\hat{B}_j(\omega_k,\omega_L)\ \Delta_o^2 = \frac{4M^2}{3M^2+1} \frac{1}{n} \sum_{s=o}^{n-1} x^{\omega_k}(s)\ \tilde{x}^{\omega_L}(s)\ x^{\omega_k+\omega_L}(s)$$

It is easy to see that this gives exactly same results as the straight forward evaluation of operation 4(a) or (b) respectively and this is more economical since one does not have to compute $\tilde{X}$ and $\tilde{x}$.

The third window which is to be discussed is a good window. A good window is one which satisfies the following requirements:

i) The variance of the estimate is as small as possible.

ii) The width of the window must be as small as possible to reduce the computing costs

iii) The window must be concentrated near the origin to reduce the bias of the estimate.

The window to be discussed is optimum in the sense that the bias of the estimate obtained by using this window is the minimum possible[5]. The variance of the estimate and computing costs are approximately the same in all the three cases. This optimum window in the time domain can be expressed as follows:

$$\omega_o(\tau_1, \tau_2) = d_o(\tau_1)\ d_o(\tau_2)\ d_o(\tau_2-\tau_1)$$

where $d_o(\tau) = \frac{1}{\pi} |\mathrm{Sin}(\pi\tau/M)| + (1 - \frac{|\tau|}{M})\cos(\pi\tau/M)$

and the corresponding expression in frequency domain is as follows:

$$W_o(\omega_1, \omega_2) = \frac{1}{2\pi} \int_{-\infty}^{\infty} D_o(\omega_1 - y)\, D_o(\omega_2 + y)\, D_o(y)\, dy$$

where $D_o(\ ) = 4M\pi^2 \dfrac{1+\cos M}{(M^2\omega^2 - \pi^2)^2}$

where M is the maximum time lag of the window.

This window is used for estimating the bispectral density in this work.

Thus we have discussed the principle behind bispectral holography and estimation of bispectral density in this chapter.

CHAPTER 4

COMPUTER SIMULATION OF THE IMAGING MODEL

In the previous chapter the methodology for recording the hologram using bispectral analysis, and the computational aspects involved in the estimation of the bispectra were discussed. In this chapter the simulations that have been carried out for imaging the objects using bispectral analysis are given.

4.1 Image Reconstruction of a Point Source

The model used for computer simulation is shown in Fig. 4.1. Here the object considered is a point source. The signal emitted by the object is

$$S(t) = a_1 \cos(\omega t + \varphi) + a_2 \cos(2\omega t + \varphi) + a_3 \cos(4\omega t + \delta(t)) \qquad (4.1)$$

where $\delta(t)$ is randomly fluctuated in time with uniform distribution over the range $(-\pi$ to $\pi)$. The signal chosen above is quasi-periodic, zero-mean and non-Gaussian. The noise that is added to the signal at the receivers is assumed to be Gaussian. The computer generated pseudo white Gaussian signal is taken as noise. The results of simulation for the power spectrum and bispectrum of the signal and noise are as follows. The power spectrum and bispectrum of both the signal and noise are computed. They are shown in Fig. 4.2, Fig.4.3 and Fig.4.4. The Figs. 4.3 and 4.4 are

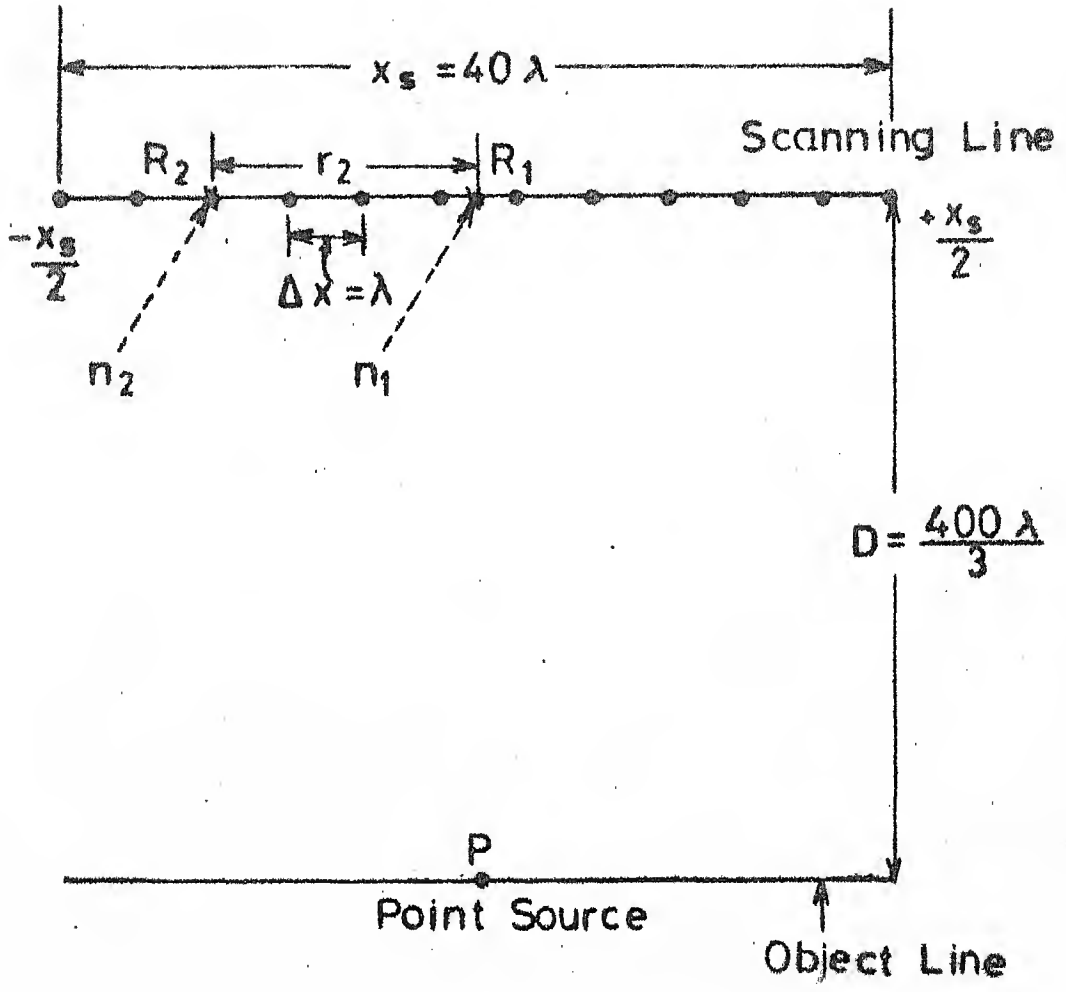

FIG. 4·1 SET UP USED FOR THE RECONSTRUCTION OF THE IMAGE OF A POINT SOURCE

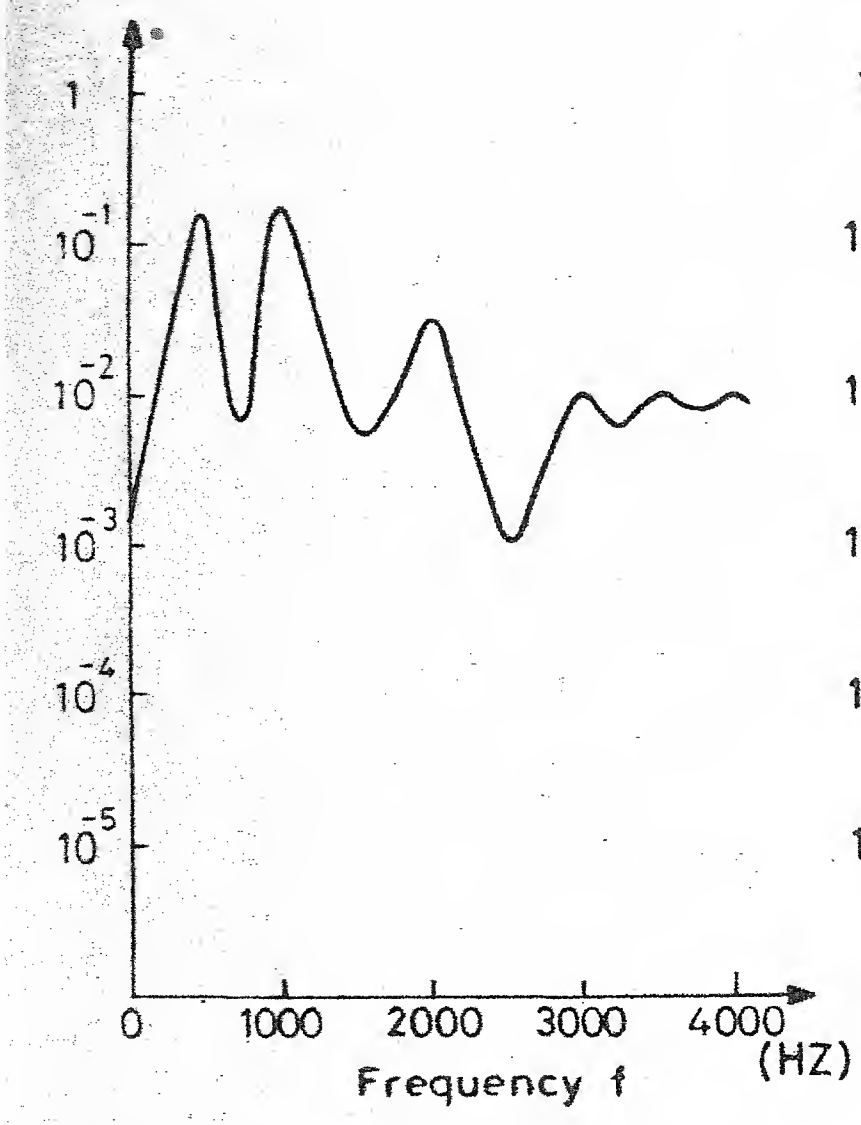

FIG. 4·2a POWER SPECTRAL DENSITY OF THE QUASI PERIODIC NON-GAUSSIAN SIGNAL

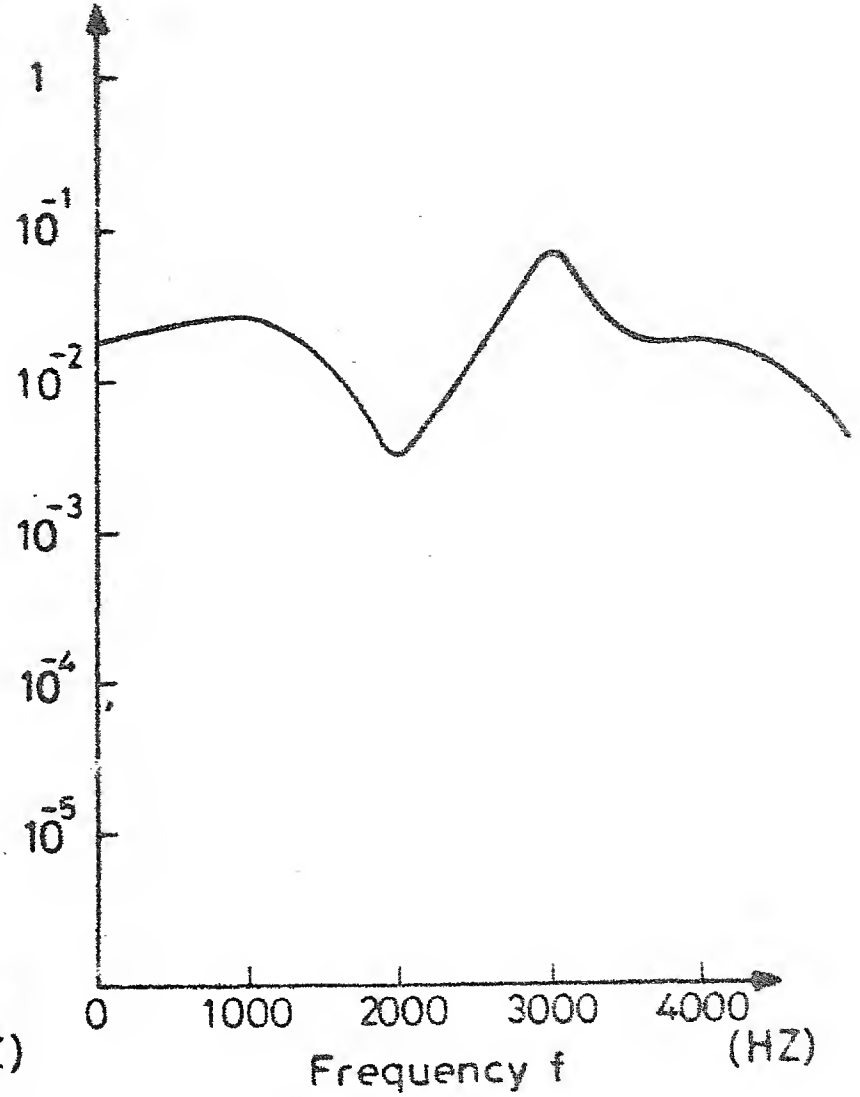

FIG. 4·2b POWER SPECTRAL DENSITY OF THE COMPUTER GENERATED GAUSSIAN NOISE

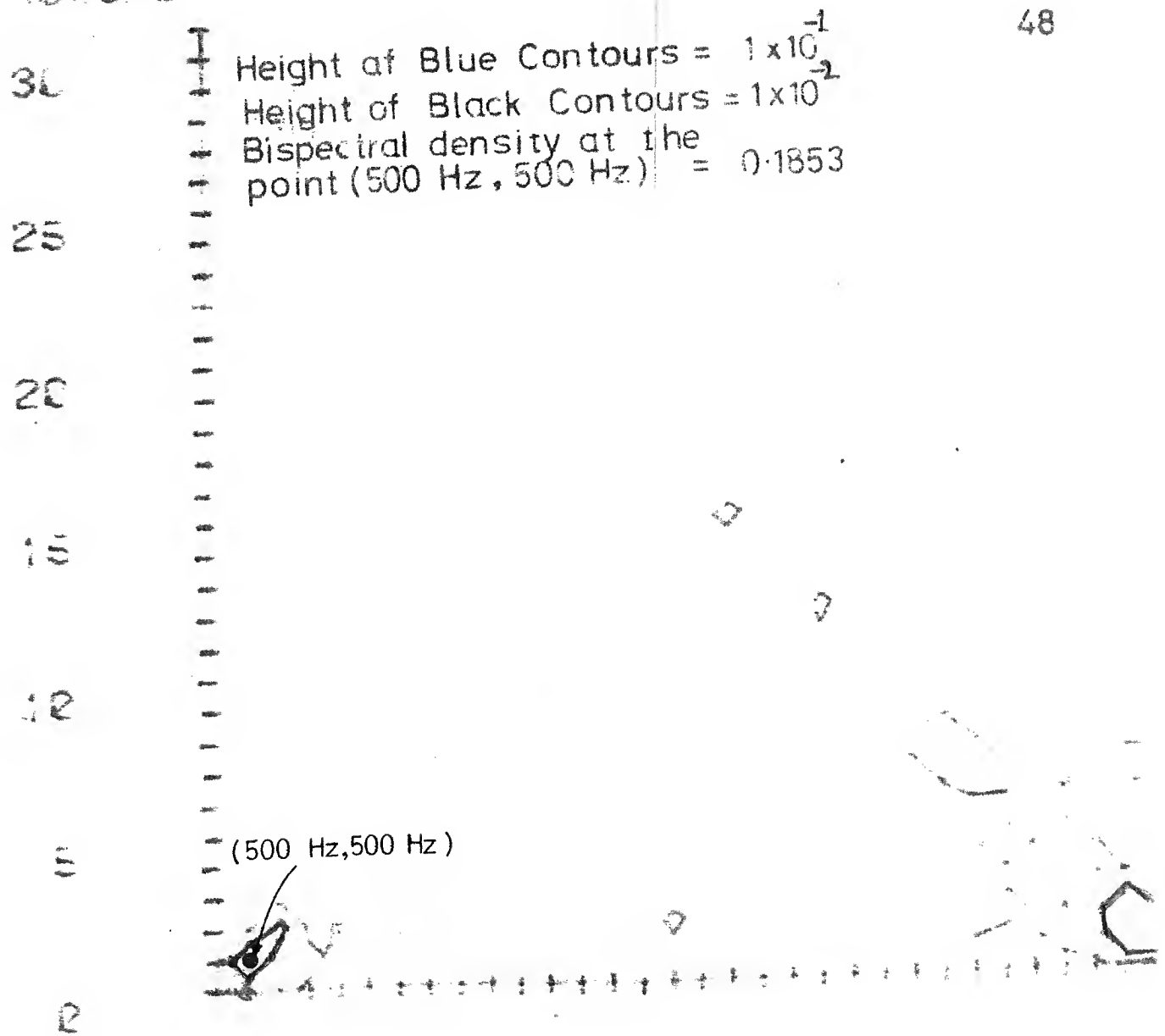
X500HZ
Height of Blue Contours = 1×10^{-1}
Height of Black Contours = 1×10^{-2}
Bispectral density at the point (500 Hz, 500 Hz) = 0·1853
35
25
20
15
12
5
2
(500 Hz,500 Hz)

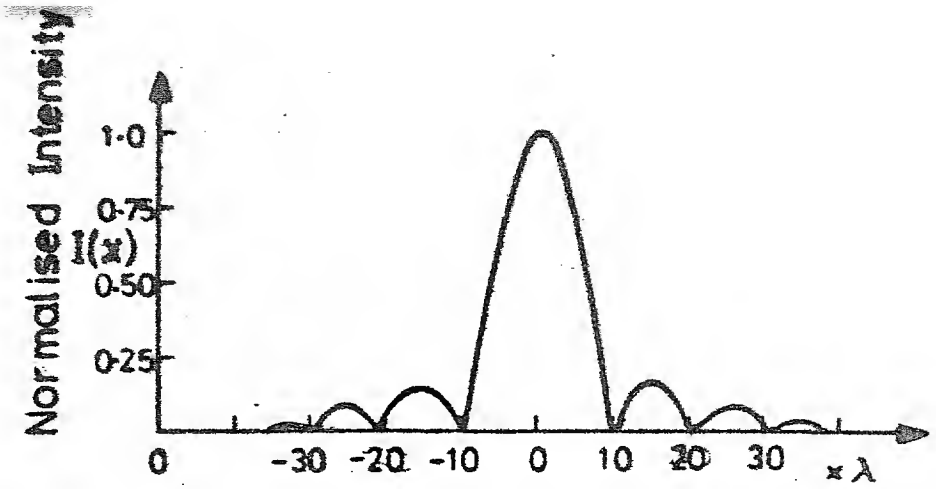

FIG. 4·5 (a) RECONSTRUCTED IMAGE OF A POINT SOURCE

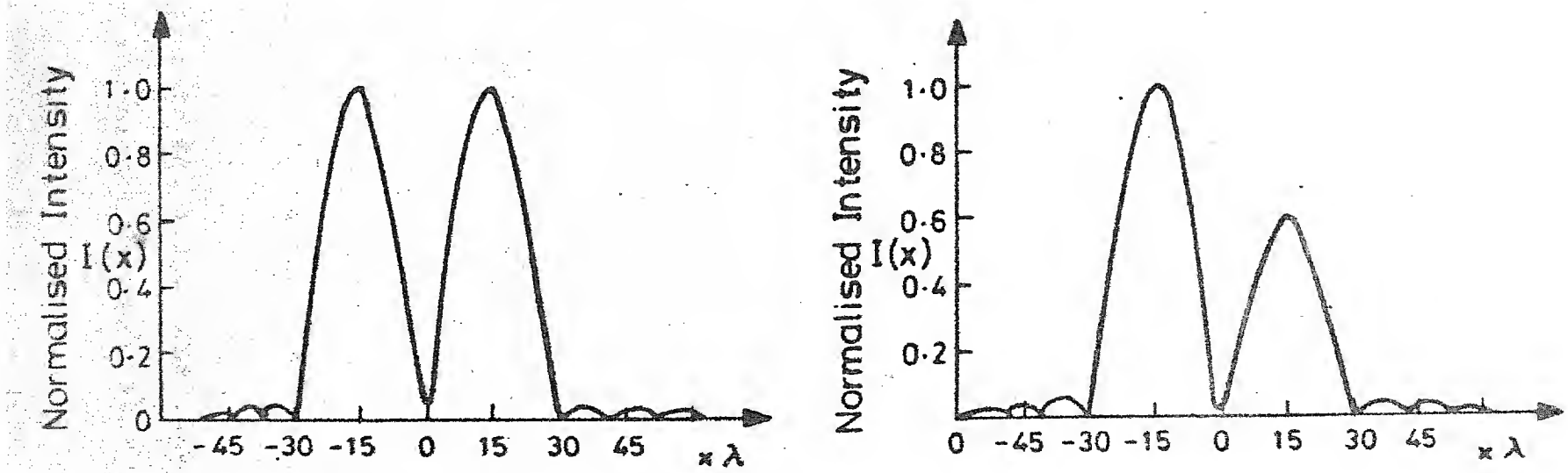

FIG. 4·5 (b) RECONSTRUCTED IMAGES OF TWO POINT SOURCES

4.2 Image Reconstruction of Two Adjacent Point Sources

The model used for simulation is similar to the one shown in Fig. 4.1, except for the fact that, two point sources are considered in the object plane instead of one. These two point sources are separated by a distance more than the resolution limit $2\lambda D/x_s$ where D is the distance of separation between the object line and scanning line. The same procedure as adapted in the case of a single point source is followed here. The reconstructed image is shown in Fig. 4.5 (b). In this figure reconstructed images for two cases are shown. In one case the two point sources are assumed to emit identical signals. In the other case it is assumed that the signals emitted by the two point sources are assumed to have different amplitude distributions. It is observed that the spacing between the two point sources in the reconstructed image is same as the spacing between the two point objects.

4.3 Image Reconstruction of an 'Uniformly Illuminated Patch'

The hologram considered here is a two dimensional one. Here also two detectors are employed, one fixed at the origin and the other scanning the hologram plane. The set up for this is shown in Fig. 4.6. The signal x(t) emitted by the object is expressed as in Eq.(4.1). The contribution of the object signal to the signal detected at a point r

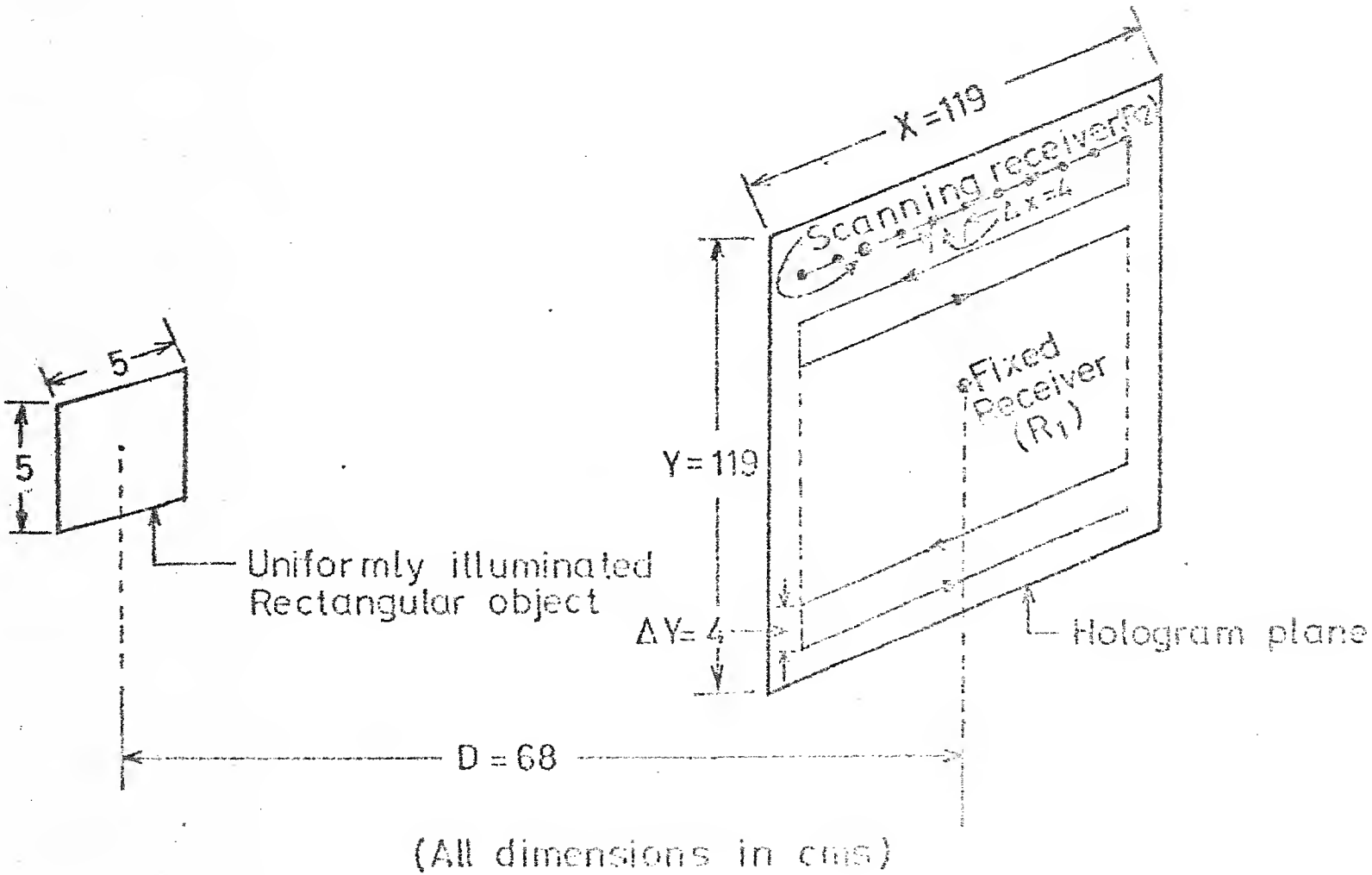

FIG. 4·6 SET UP USED FOR THE IMAGE RECONSTRUCTION OF A "UNIFORMLY ILLUMINATED RECTANGULAR PATCH"

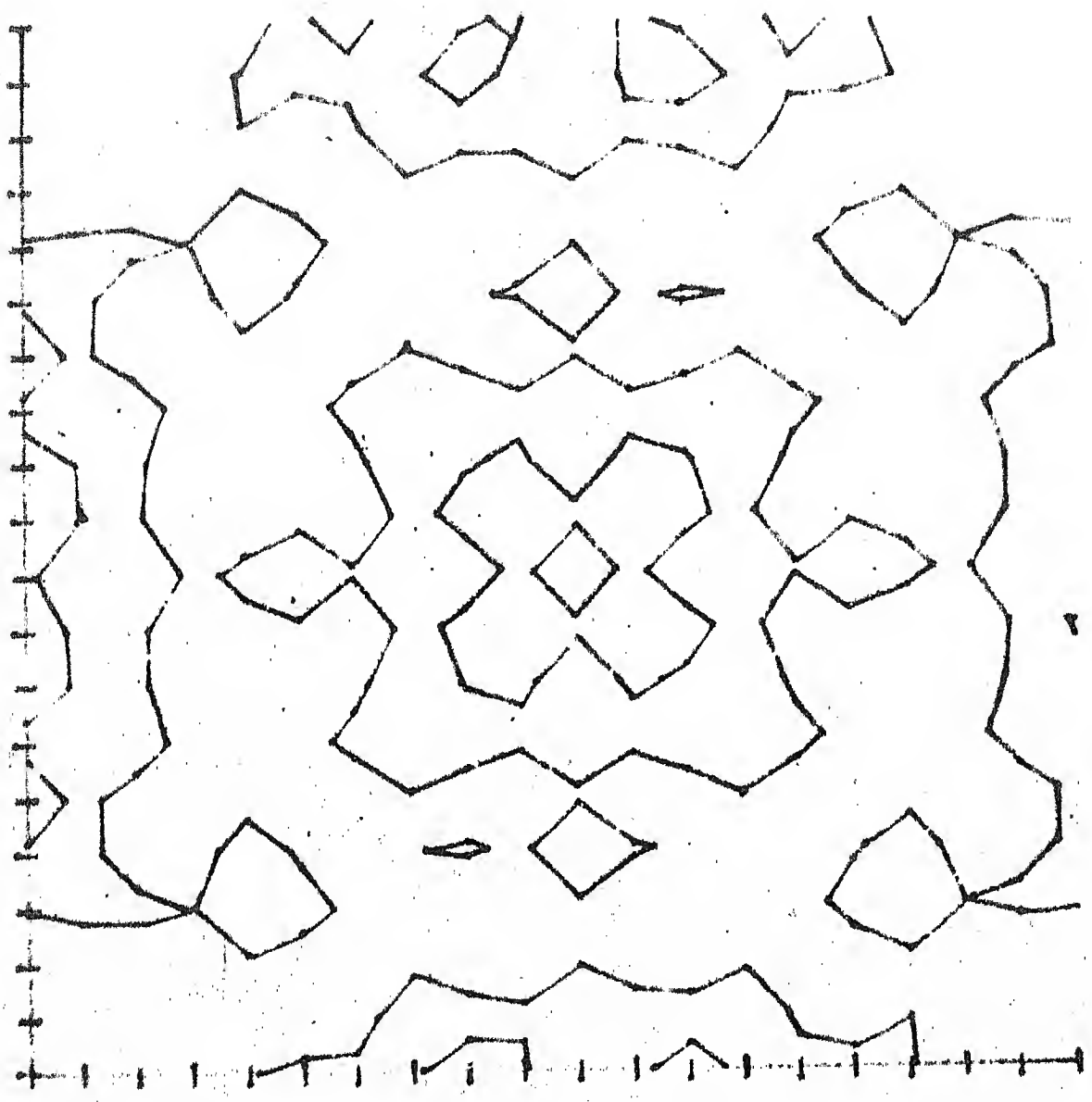

Fig 4.7 RECONSTRUCTED IMAGE OF THE OBJECT

"UNIFORMLY ILLUMINATED OBJECT"

on the hologram plane is obtained by integrating x(t) over the whole object. As it takes more time to compute the integral, to find out the signal contribution the object is considered as a matrix (5 x 5) of point sources. Because of this fact the reconstructed image has slight intensity variations. The reconstructed image is shown in Fig. 4.7. It is obtained by contour mapping. All the contours shown in the figure correspond to same height. Since the variations in the intensities are very small, the contour of chosen intensity appear as shown in the figure. It is not giving a clear indication of the object. Because of that the reconstructed values of the Image are also given in Tab. 4.1 which clearly gives the intensity variations.

In all the above cases, the medium considered causes only linear phase shift and attenuation.

The signal processing steps involved in the data acquisition and computer simulation of bispectral imaging technique are illustrated in Fig. 4.9.

Table 4.1

RECONSTRUCTED VALUES OF THE IMAGE

3.41	2.90	2.62	3.11	3.65	3.88	2.55	3.48	2.76	4.14	2.96	4.40	2.75	3.48	4.05	4.12
4.14	2.53	3.35	3.65	2.54	4.43	4.16	4.22	2.50	4.50	3.74	4.17	2.85	3.07	3.08	4.28
4.41	3.00	2.52	3.00	2.52	4.19	3.87	4.32	3.88	4.38	4.37	4.13	2.94	2.66	4.61	3.97
3.90	2.73	2.64	4.11	3.79	3.46	3.78	2.62	3.42	4.29	3.32	4.33	3.98	3.92	3.20	2.55
3.98	3.36	2.60	4.22	3.27	4.10	3.39	4.29	4.17	4.18	2.63	4.10	3.44	3.57	2.80	3.73
4.29	3.70	4.15	3.42	4.07	4.23	3.65	3.33	3.04	3.36	3.18	4.50	3.07	3.17	2.93	4.20
3.75	3.40	4.44	3.80	2.63	2.70	2.72	4.29	3.40	2.75	3.50	4.07	3.46	2.56	2.75	3.57
3.66	3.47	3.74	3.40	2.82	3.35	4.14	4.01	3.51	3.55	3.10	3.22	4.31	2.90	3.53	3.41
4.36	3.30	4.01	4.02	4.32	4.08	4.34	4.22	2.79	3.53	2.78	3.95	2.55	2.92	3.37	2.60
4.00	2.96	3.79	2.86	4.41	2.53	4.28	2.71	3.00	2.73	3.34	3.13	4.05	2.60	3.80	3.25
3.65	3.03	2.61	2.91	3.90	3.11	3.98	3.41	4.21	4.24	2.84	3.12	3.21	3.85	2.70	2.70
4.15	3.17	3.89	2.98	4.03	2.89	2.67	3.33	3.35	2.60	2.55	4.26	3.09	2.93	3.83	3.85
3.69	2.75	4.24	3.46	2.68	3.09	2.75	3.70	4.06	3.20	3.21	3.29	3.76	2.86	4.02	3.29
2.87	3.01	3.57	2.62	4.12	4.45	3.45	2.61	2.56	2.59	2.95	3.27	4.53	3.30	4.63	4.46
3.31	2.77	3.43	3.33	4.33	3.97	4.24	4.29	3.72	4.13	2.80	3.14	4.10	3.27	4.51	3.05
3.32	3.06	3.23	3.58	3.87	3.92	3.81	2.56	2.59	2.80	4.09	3.62	3.09	4.23	3.59	2.57
3.50	3.73	4.27	3.72	4.00	2.52	3.79	2.75	3.43	3.49	4.47	3.44	3.68	3.61	3.48	3.71
3.45	4.11	3.37	3.78	4.23	3.68	4.13	2.50	3.17	3.49	4.04	2.55	3.27	3.17	3.79	3.27
3.94	3.05	2.79	2.56	4.43	3.53	3.03	4.33	2.76	3.59	4.05	3.74	4.20	3.63	4.20	3.58
2.84	2.54	2.57	4.00	2.52	4.12	4.33	2.91	3.79	3.13	2.63	3.18	3.68	2.58	4.27	3.11

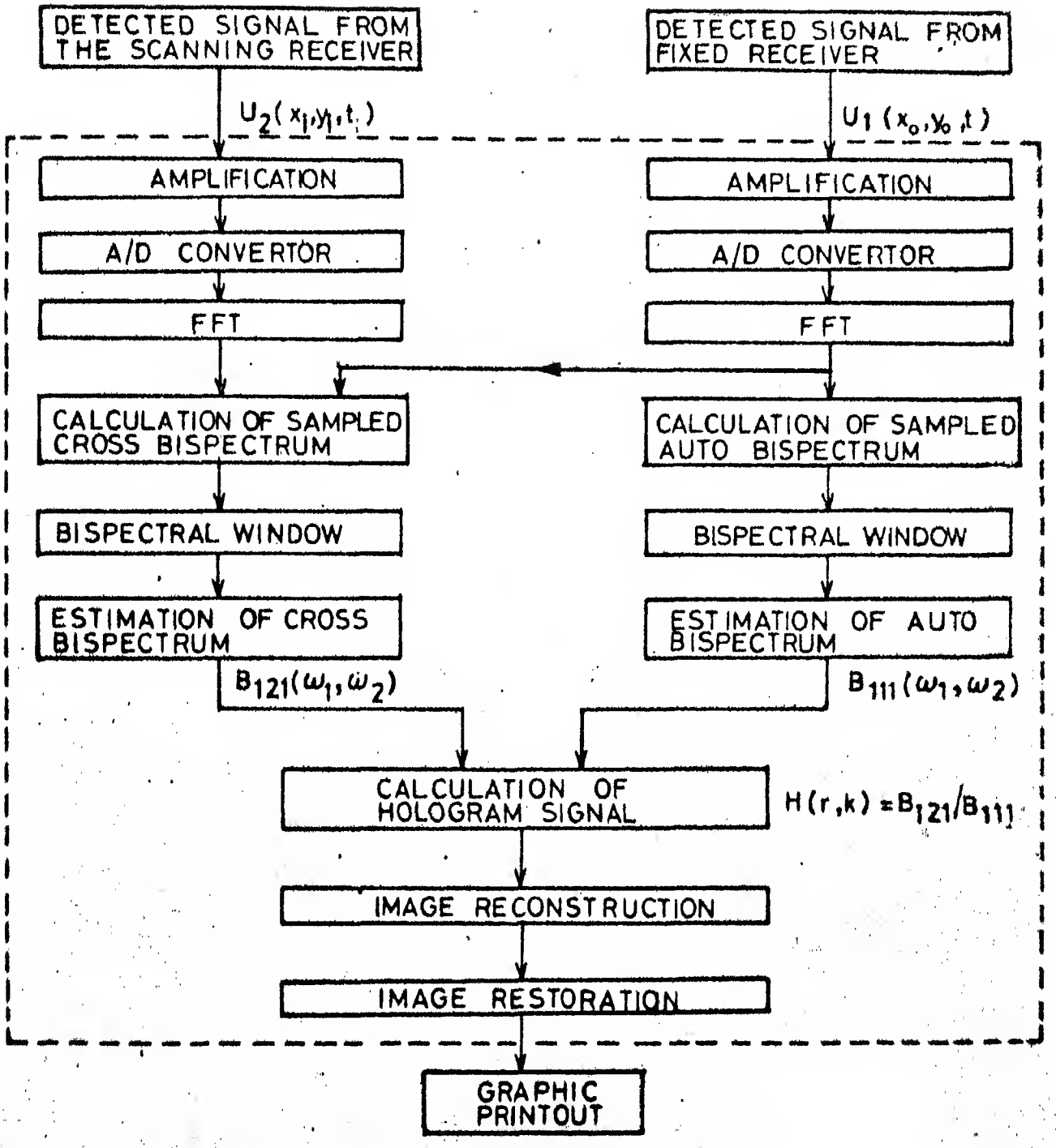

FIG.4·9 SIGNAL PROCESSING STEPS IN BISPECTRAL HOLOGRAPHY

CHAPTER 5

CONCLUSIONS AND SUGGESTIONS

A study of the paper titled 'Bispectral Holography' by Takuso Sato and Kimio Sasaki initiated this work. After a brief discussion of the principles of holography and differences between the optical and acoustical holography, the technique of 'bispectral holography' as proposed by Sato and Sasaki is examined. A survey of the work carried out in this area is done. The fact that 'the bispectral analysis can eliminate the effects of noise and channel on the signal completely' is re-established using computer simulation with the help of three examples. In this work the channel is assumed to be 'deterministic'. Because of the immediate nonavailability of the information on realistic models of randomly turbulent media, no example pertaining to this case could be included, though the theory applies to this media also. This technique naturally requires more computation time than the conventional technique as one has to compute both the cross- and auto-bispectral densities of the scanned and reference signals and their ratio whereas in the conventional method one has to compute only the cross-power spectral density between the scanned and reference signals, for getting the hologram signal, but the advantages gained clearly justify the increased computation.

5.1 Suggestions for Future Work

Apart from its current applications to acoustic imaging, passive sonar [6] and machine system diagonosis [7], it is felt that the technique can be applied to problems of channel characterization and communications. This is elaborated in the following discussion.

a) Channel Characterization:

The procedure for channel characterization using the present method is as follows. A zero mean, non-Gaussian signal is transmitted through the channel to be characterized. Assume the corrupting noise to be additive Gaussian and statistically independent of the signal. The bispectrum of the received signal will be the bispectrum of the channel corrupted transmitted signal as the bispectrum of the noise becomes zero. The mathematical procedure for finding out the transfer function of the channel from the bispectrums of the transmitted and received signals is given below.

Let $h(t,\tau)$ be the impulse response of the linear time varying channel to be characterized. A known signal $x(t)$ is transmitted through the channel. It is assumed to be a quasi-periodic, non-Gaussian zero mean process. Its third order correlation function is assumed to be ergodic. The bispectral density of $x(t)$ is obtained by observing the signal $x(t)$ over a period T (T is sufficiently large to satisfy the ergodicity property and is given by

$$B_x(\omega_k, \omega_L) = \frac{1}{T} X(\omega_k)\, X(\omega_L)\, X^*(\omega_k + \omega_L) \qquad (5.1)$$

The signal received at the other end of the channel is given by

$$Y(t) = \int_{-\infty}^{\infty} x(\tau)\, h(t,\tau)\, d\tau + n(t)$$

$$= m(t) + n(t)$$

Assuming that Y(t) is zero mean and its third order correlation function is ergodic, $R_y(\tau_1, \tau_2)$ is expressed as

$$\frac{1}{T} \int_0^T y(t)y(t+\tau_1)y(t+\tau_2)$$ (Assuming T is sufficiently large to satisfy the ergodicity property)

$$= \frac{1}{T} \int_0^T m(t)\, m(t+\tau_1)\, m(t+\tau_2)$$ (This is true under the assumption that m(t) and n(t) are statistically independent).

$$\therefore B_y(\omega_k, \omega_L) = \frac{1}{T} M(\omega_k)\, M(\omega_L)\, M^*(\omega_k+\omega_L)$$

$$= \frac{1}{T} X(\omega_k)\, H(\omega_k, \tau)\, X(\omega_L)\, H(\omega_L, \tau)\, X^*(\omega_{k+L})$$

$$H^*(\omega_{k+\omega_L}, \tau) . \qquad (5.2)$$

(Assuming that the channel is not varying over the interval of observation) where τ is any time instant in the interval T. The ratio of Eqs.(5.1) and (5.2) gives

$$B_H(\omega_k, \omega_L, \tau) = H(\omega_k, \tau)\, H(\omega_L, \tau)\, H^*(\omega_k + \omega_L, \tau)$$

Evaluate $B_H(\omega_k, \omega_L, \tau)$ for $k, L = 1, 2, \ldots n$.

Then arranging these values in matrix form

$$\begin{bmatrix} H(\omega_1,\tau)H(\omega_1,\tau)H^*(\omega_1+\omega_1,\tau) \cdots & H(\omega_1,\tau)H(\omega_n,\tau)H^*(\omega_n+\omega_1,\tau) \\ H(\omega_2,\tau)H(\omega_2,\tau)H^*(\omega_2+\omega_2,\tau) & \\ H(\omega_n,\tau)H(\omega_1,\tau)H^*(\omega_n+\omega_1,\tau) & H(\omega_n,\tau)H(\omega_n,\tau)H^*(\omega_n+\omega_n,\tau) \end{bmatrix}$$

$$= \begin{bmatrix} B_H(\omega_1,\omega_1,\tau) & B_H(\omega_1,\omega_2,\tau) & B_H(\omega_1,\omega_n,\tau) \\ & B_H(\omega_2,\omega_2,\tau) & \\ B_H(\omega_n,\omega_n,\tau) & & B_H(\omega_n,\omega_n,\tau) \end{bmatrix}$$

To solve for $H(\omega_1,\tau)$, $H(\omega_2,\tau)$.....$H(\omega_{2n},\tau)$ there are only $\frac{n(n+1)}{2}$ equations since the above matrix is a symmetric matrix.

Since the above system is an over determined system of non-linear equations with multiplicative terms to find a solution one will have to first linearize them by taking the logarithm and then resorting to any one of the methods of solution for over determined system, e.g. pseudo inverse [16], least squares or residual projection method [17].

b) Communication through a Randomly Time Varying Media:

The image of the object reconstructed using bispectral analysis has the effect of neither the channel nor the additive

Gaussian noise. The bispectral analysis may be applied in the communications context where the aim is to obtain the signal free from additive noise and the effects of the channel. To get the image of the object the variation of the amplitude and phase of the object wave relative to those of the reference wave in space has to be determined whereas to get the signal transmitted, the variation of the amplitude and phase of the object signal with time has to be determined. For obtaining the signal, an analysis similar to the one used for getting image of the object can possibly be carried out by interchanging time and space domains.

APPENDIX

This contains some of the important listings of the computer simulation. Comment cards introduced in ach routine explains the function of that routine.

REFERENCES

1. B.P. Hildebrand and B.B. Brebden, 'An Introduction to Acoustical Holography', Plenum, New York, 1972.

2. Takuso Sato, Kimio Sasaki, 'Bispectral Holography', Journal of Acoustical Society of America, Vol.62, No.2, August 1977, pp. 404-408.

3. P.J. Huber, B.Kleiner, T. Gasser and G. Dummermuth, 'Statistical Methods for Investigating Phase Relations in Stationary Stochastic Process', IEEE Transactions on Audio and Electroacoustics, Au-19, 1971, pp. 78-86.

4. D.R. Brillinger, 'An Introduction to Polyspectra', Ann. Math. Stat. 36, 1965, pp. 36-46.

5. K. Sasaki, T. Sato and Y. Yamashita, 'Minimum Bias Windows for Bispectral Estimation', Journal of Sound and Vibrations- 40, 1975, pp. 139-148.

6. Kimio Sasaki, Takuso Sato and Yoichi Nakumura, 'Holographic Passive Sonar', IEEE Transactions on Sonics and Ultrasonics, Vol. SU-24, No.3, May 1977, pp. 193-200.

7. Takuso Sato, Kimio Sasaki and Masaharu Nonaka, 'Prototype of Bispectral Passive Imaging Systems Aiming Machine-System Diagonsis', Journal of Acoustical Society of America, 63(5), May 1978, pp. 1611-1616.

8. J.W. Vanness, 'Asymptotic Normality of Bispectral Estimates', Annals of Mathematical Statistics 37, 1966, pp. 1257-1272.

9. J.W. Goodman, 'Introduction to Fourier Optics', McGraw-Hill, New York, 1968, Chapter 8.

10. W.T. Cathey, 'Optical Information Processing and Holography', John Wiley and Sons, New York.

11. R.K. Otnes, L. Enochson, 'Applied Time Series Analysis', Vol.1, Wiley - Interscience Publication, New York.

12. V.I. Tatarski, 'Wave Propagation in a Turbulent Medium', Dover Publications, Inc. New York.

13. A. Gersho, 'Characterization of Time Varying Linear Systems', Research report, School of Electrical Engineering, Cornell University, Feb. 1963.

14. KimioSasaki and Takuso Sato, 'A Bispectral Synthesizer', Journal of Acoustical Society of America 65(3), March 1979.

15. Kimio Sasaki, Takuso Sato and Yoichi Nakumuru, 'An Effective Utilization of Spectral Spread in Holographic Passive Imaging Systems', IEEE Transactions on Sonics and Ultrasonics, Vol.Su-25, No.4, July 1978.

16. C.R. Rao and S.K. Mitra, 'Generalized Inverse of Matrices and its Applications', John Wiley and Sons, Inc., New York, 1971.

17. K. Tanabe, 'Projection Method for Solving a Singular System of Linear Equations and its Applications', Numerische Mathematik, 17, pp. 203-214, 1971.

18. Akira Ishimaru, 'Theory and Applications of Wave Propagation and Scattering in Random Media', Proceedings of the IEEE, July 1977, pp. 1030-1059.

19. E.V. Hoversten, R.O. Harger and S.J. Halme, 'Communication Theory for the Turbulent Atmosphere', Proceedings of IEEE, Special Issue on Optical Communication, Oct. 1970. pp. 1626-1649.

20. Anthony J. Devaney, 'Optical Coherence: Self-perpetuating Science', Optical Spectra, Oct. 1979, pp. 37-41.

```
C     ***************************************************************
C     A PROGRAMME FOR OBTAINING THE IMAGE OF A POINT SOURCE
C     ***************************************************************
      DIMENSION X1(32),Y1(32), X(32),Y(32),INK(5)
      DIMENSION INK1(390),LD(390),WK(390),XIMA(40)
      COMPLEX ABSD(41),CBSD(41),HS(41)
      COMPLEX GAMN,Z(32),HOSI,Z1(32),RIMA(-20:19)
      N=32
      PI=3.1415926535
      R1=-PI
      R2=PI
      SP=2.0
      PHI=0.52359
      N1=N/2
      F=10000
      V=33000
200   FORMAT(5X,'AUTOBISPECTRAL DENSITY',//)
210   FORMAT(5X,'CROSS BISPECTRAL DENSITY',//)
220   FORMAT(5X,'HOLOGRAM SIGNAL',//)
100   FORMAT(5X,'SAMPLED VALUES OF THE SIGNAL IN THE TIME DOMAIN',//)
110   FORMAT(5X, 8F15.8,//)
120   FORMAT(5X,'FIRST N/2 FOURIER COEFFICIENTS OF THE SIGNAL',//)
130   FORMAT(5X,'N/2+1TH FOURIER COEFFICIENT OF THE SIGNAL',//)
140   FORMAT(5X,'POWER SPECTRAL DENSITY OF COMPUTER GENERATED
     1NOISE',//)
150   FORMAT(5X,'SAMPLED VALUES OF THE BISPECTRAL DENSITY OF
     1THE COMPUTER GENERATED NOISE',//)
116   FORMAT(5X,'POWER SPECTRAL DENSITY OF THE GIVEN QUASI PERIODIC
     1NONGAUSSIAN SIGNAL',//)
117   FORMAT(5X,'BISPECTRAL DENSITY OF THE GIVEN QUASI
     1PERIODIC NONGAUSSIAN SIGNAL'//)
111   FORMAT(1X,10(1X,4(2F15.8)))
112   FORMAT(1X,10(5X,4(2F15.8)))
113   FORMAT(1X,10(9X,4(2F15.8)))
250   FORMAT(//,1X,'ROW NO',I3,//)
C     ***************************************************************
C     THE OBJECT WE ARE CONSIDERING HERE IS A POINT SOURCE
C     ***************************************************************
C     DISTANCE BETWEEN THE OBJECT AND HOLOGRAM PLANE D=6SCM
C     ***************************************************************
C     SIGNAL EMITTED BY THE OBJECT IS X(T)=COS(WT+PHI)+COS(2*WT+PHI)
C    *+COS(4*WT+PHI)
C     ***************************************************************
C     SCANNING RANGE IS (-20*PLAMDA TO +20*PLAMDA); SCANNING
C     INTERVAL PLAMDA
C     ***************************************************************
C     DISTANCE BETWEEN HOLOGRAM PLANE AND OBJECT=D=100*PLAMDA/3
C     ***************************************************************
      DO 110 KK=1,3
      [illegible], PLAMDA
      D=100.00
      D=D*2
      XY=2*PI*F/V
      DSHP2=XY*D
      DO 165 K=1,41
      I=K
      IT=-20*PLAMDA+PLAMDA*(I-1)
```

```
      D2=T1**2
      DSDP1=RM*SQRT(D2+T2)
      DO 30 M=1,N
      RTM=FLOAT(M-1)/FLOAT(M)
      PHI=2*PI*RTM
      Y(M)=COS(RM-DSDP1)+COS(2*RM-2*DSDP1+PHI)
     1+COS(3*RM-4*DSDP1+PHI)
30    X(M)=COS(RM-DSDP2)+COS(2*RM+PHI-2*DSDP2)
     1+COS(3*RM+PHI-4*DSDP2)
      CALL DDD(X,GAMM,N,IWK,Z)
      CALL DDD(Y,GAMM,N,IWK,Z1)
      ABSD(K1)=Z(2)*Z(2)*CONJG(Z(3))
      CBSD(K1)=Z1(2)*Z(2)*CONJG(Z(3))
      HOST=CBSD(K1)/ABSD(K1)
      HS(K1)=HOST
165   CONTINUE
      J=0
      DO 88 I=-20,19
      J=J+1
88    RTMA(I)=CONJG(HS(J))
      CALL FFTP(RTMA,40,IWK1,WK,LL)
      PRINT400
400   FORMAT(5X,'RECONSTRUCTED VALUES OF THE SIGNAL',/)
      DO 99 I=1,40
99    XTMA(I)=CABS(RTMA(I))
      PRINT700,(XTMA(I),I=1,40)
700   FORMAT(5X,8F15.8,/)
119   CONTINUE
      STOP
      CALL FFTP
      CALL FFTR2
      CALL FFT2
      END
      SUBROUTINE DDD(X,GAMM,N,IWK,Z)
      DIMENSION X(32),IWK(6),XTMA(40)
      COMPLEX Z(32),GAMM,CMPLX
      M1=N/2
      M2=N-1
      CALL FFTR(X,GAMM,N,IWK)
      DO 90 I=1,N
90    X(I)=X(I)/N
      GAMM=GAMM/N
      K=0
      DO 90 L=1,M1,2
      K=K+1
90    Z(K)=CMPLX(X(L),X(L+1))
      DO 70 L=2,M1
70    Z(M2-L)=CONJG(Z(L))
      Z(M1)=GAMM
      DO 60 L=1,M
60    X(L)=(CABS(Z(L)))**2
      PRT 230
230   FORMAT(5X,'POWER SPECTRAL DENSITY OF THE GIVEN SIGNAL',/)
      PRT10,(X(I),I=1,N)
10    FORMAT(5X,8F15.9,/)
      RETURN
      END
```

```
C     ***********************************************************
C     A PROGRAMME FOR GENERATING THE BISPECTRAL DENSITY OF THE
C     GIVEN SIGNAL
C     ***********************************************************
      DIMENSION X(32),DD(64),TAK(6),Y(32),V(4),TO(4)
      COMPLEX Z(0:32),B(32,32),GAMM,CMPLX,Z7
      COMMON/AREA1/B
      DATA V/1.,32.,1.,32./
      DATA TO/0.5,1.1,0.3,0.9/
      N=32
      PI=3.1415926535
      H1=-PI
      H2=PI
      SP=2.0
      PHI=0.52359
      ISEED=21478364
      T=0.001/FLOAT(16)
      P=1.0/(N*T)
      N1=N/FLOAT(2)
100   FORMAT(5X,'SAMPLED VALUES OF THE SIGNAL IN THE TIME DOMAIN',//)
105   FORMAT(5X,'SAMPLED VALUESS OF THE NOISE IN THE TIME DOMAIN',//)
110   FORMAT(5X,8F15.8,//)
140   FORMAT(5X,'POWER SPECTRAL DENSITY OF THE GIVEN QUASI
     1PERIODIC NONGAUSSIAN SIGNAL',//)
145   FORMAT(5X,'POWER SPECTRAL DENSITY OF THE
     1GAUSSIAN NOISE',//)
150   FORMAT(5X,'SAMPLED VALUES OF THE BISPECTRAL DENSITY OF THE
     1THE GIVEN QUASI PERIODIC NONGAUSSIAN SIGNAL',//)
155   FORMAT(5X,'SAMPLED VALUES OF THE BISPECTRAL DENSITY OF THE
     1THE COMPUTER GENERATED NOISE',//)
410   FORMAT(5X,'ROW NO.',I3)
210   FORMAT(1X,4(2F15.6))
103   FORMAT(5X,'SIGNAL TO NOISE RATIO=',//)
C     ***********************************************************
C     GENERATING THE SAMPLED VALUES OF THE NOISE IN THE TIME
C     DOMAIN
C     ***********************************************************
      CALL GGNMP(ISEED,N,Y)
      DO 333 I=1,N
333   Y(I)=1.00*Y(I)
      TYPE105
      TYPE110,(Y(I),I=1,N)
C     ***********************************************************
      CALL FFT(Y,Z,GAMM,N,IRK)
      TYPE 145
      TYPE110,(Y(I),I=1,N)
      CALL BSD(Z,N)
      TYPE 155
      DO 232 I=1,N
      TYPE410,I
232   TYPE210,(B(I,J),J=1,N)
      CALL [illegible](3)
      CALL VPORT(TO)
      CALL [illegible](V)
      CALL [illegible](N)
      STOP
      CALL [illegible]
```

```
      CALL ERROR2
      CALL FFT2
      END
      SUBROUTINE FFT(X,Z,GAMN,N,IWK)
C     ***************************************************************
C     THIS SUBROUTINE COMPUTES THE POWER SPECTRAL DENSITY
C     ***************************************************************
      DIMENSION X(32),IWK(6)
      COMPLEX Z(0:32),R,GAMN
      CALL FFTR(X,GAMN,N,IWK)
      DO 11 I=1,N
11    X(I)=X(I)/N
      GAMN=GAMN/N
      K=0
      M1=N-1
      N1=N/2
      DO 20 I=1,M1,2
      K=K+1
20    Z(K)=CMPLX(X(I),X(I+1))
      DO 30 I=2,N1
30    Z(N+2-I)=CONJG(Z(I))
      Z(N1+1)=GAMN
      DO 40 I =1,N
40    X(I)=(CABS(Z(I)))**2
      RETURN
      END
      SUBROUTINE BSD(Z,N)
C     ***************************************************************
C     GENERATING THE SAMPLED BISPECTRUM OF THE SIGNAL IN THE
C     FREQUENCY DOMAIN
C     ***************************************************************
      COMPLEX Z(0:32),B(32,32)
      COMMON/AREA1/B
      N1=N-1
      DO 310 I=1,N
310   Z(I-1)=Z(I)
      IP1=0
      JP1=0
      DO 55 J=0,N1
      JP1=JP1+1
      DO 50 I=1,J
      IP1=IP1+1
      IR=I+J
      IF (IR.LT.N) GO TO 4
      IR=IR-N+2
4     ZZ=Z(I)*Z(J)
      B(IP1,JP1)=CABS(ZZ*CONJG(Z(IR)))
50    CONTINUE
      IP1=0
55    CONTINUE
      RETURN
      END
      SUBROUTINE PLOTER(N)
      COMPLEX B(32,32)
      COMMON/AREA1/B
      COMMON/COAXES/NDIVX,NDIVY,IPORN(3),NOCX,NOCY
     1,CHS,CHSD,FACX,FACY,DUMMX,DUMMY
```

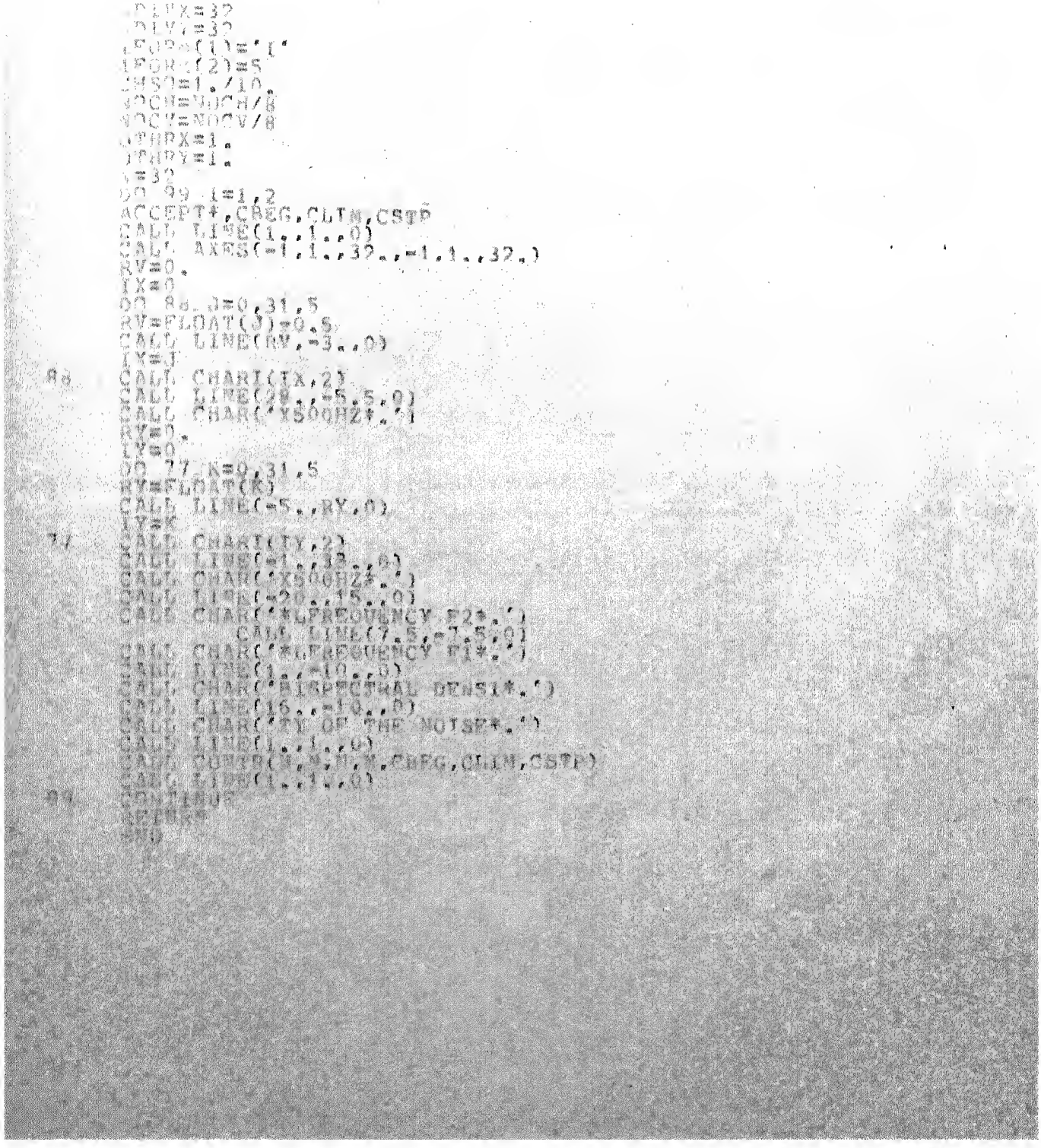

```
      DIMX=32
      DIMY=32
      LSUB=(1)='('
      LFOR=(2)=5
      XMSQ=1./10.
      NOCH=NUCH/8
      NOCV=NOCV/8
      ITHRX=1.
      ITHRY=1.
      N=32
      DO 99 I=1,2
      ACCEPT*,CBEG,CLIM,CSTP
      CALL LINE(1,1,0)
      CALL AXES(-1.1,.32.,-1.1,.32.)
      RV=0.
      IX=0
      DO 88 J=0,31,5
      RV=FLOAT(J)-0.5
      CALL LINE(RV,-3.,0)
      IX=J
   88 CALL CHARI(IX,2)
      CALL LINE(28.,-5.5,0)
      CALL CHAR('X500HZ*.')
      RY=0.
      IY=0
      DO 77 K=0,31,5
      RY=FLOAT(K)
      CALL LINE(-5.,RY,0)
      IY=K
   77 CALL CHARI(IY,2)
      CALL LINE(-1.,33.,0)
      CALL CHAR('X500HZ*.')
      CALL LINE(-20.,15.,0)
      CALL CHAR('*LFREQUENCY F2*.')
           CALL LINE(7.5,-7.5,0)
      CALL CHAR('*LFREQUENCY F1*.')
      CALL LINE(1.,-10.,0)
      CALL CHAR('RISPECTUAL DENSI*.')
      CALL LINE(16.,-10.,0)
      CALL CHAR('TY OF THE NOISE*.')
      CALL LINE(1.,1.,0)
      CALL CONTR(M,M,M,M,CBEG,CLIM,CSTP)
      CALL LINE(1.,1.,0)
   99 CONTINUE
      REPEAT*
      END
```

```
      SUBROUTINE CONTR(NDIM1,NDIM2,NUSD1,NUSD2,CSEG,CLIM,CSTP)
C     FITS CONTOURS OF SPECIFIED HEIGHTS FROM GIVEN TWO-DIMENSIONAL
C     ARRAY DATA.
C     CONTOUR HEIGHTS PLOTTED ARE CTR=CSEG,CSEG+STEP,CSEG+2*STEP,
C     ... SO LONG AS CTR DOESNOT EXCEED CLIM EITHER WHILE INCREASING OR
C     DECREASING. STEP IS CSTP WITH THE SIGN OF CLIM-CSEG. ONLY
C     CTR=CSEG IS PLOTTED IF CSTP=0.
C     DATA WAS DIMENSIONED NDIM1 BY NDIM2 IN A DIMENSION STATEMENT IN
C     THE CALLING PROGRAM,BUT ONLY THE FIRST NUSD1 BY NUSD2 ARE
C     ACTUALLY USED.(FIRST SUBSCRIPT MUST INCREASE FASTEST IN STORAGE
C     ORDER,AS USUAL). ALL ACTUAL PLOTTING IS DONE IN THE USER-
C     SUPPLIED SUBROUTINE CPLOT,WHICH MUST BE HEADED AS FOLLOWS--
C     SUBROUTINE CPLOT(IPLOT,X1,X2,CTR)
C     CONTR EXTRUDES ONE POINT AT A TIME TO CPLOT.(X1,X2) IS THE
C     COORDINATE PAIR,X1 FROM 1.0 TO FLOAT(NUSD1),X2 FROM
C     1.0 TO FLOAT(NUSD2). IF DESIRED FOR EFFICIENCY,CPLOT MAY
C     SAVE UP POINTS IN A WORK ARRAY.
C     FOR IPLOT=0,CPLOT SHOULD JUST REMEMBER THIS POINT (MOVE TO
C     (X1,X2) WITH PEN UP FOR A CALCOMP PLOTTER).
C     FOR IPLOT=1,CPLOT SHOULD DRAW A LINE SEGMENT FROM THE LAST POINT
C     TO THE CURRENT POINT AND REMEMBER THE CURRENT POINT (MOVE TO
C     (X1,X2) WITH PEN DOWN).
C     FOR IPLOT=2,CPLOT SHOULD PLOT A NUMERIC LABEL GIVING THE VALUE
C     OF CTR AT THIS POINT. EACH PHYSICALLY SEPARATE CONTOUR DRAWN
C     WILL RECEIVE ONE LABEL.
C     EACH DATUM IS INCREASED BY 1.E-20 AND ALTERED IN ITS TWO LOW ORDER
C     BITS. NON-ZERO FLOATING POINT VALUES ARE HARDLY AFFECTED,THOUGH
C     FIXED POINT VALUES MIGHT BE.(CONVERT TO FIXED POINT BY SAYING--
C     INTEGER DATA,CTRM,CTRZ,CTRD
C     AND CHANGING ABS(DATA...) TO IABS(DATA...).)
      DIMENSION NUSD(2),IX(2),IA(2),IB(2),IDELT(2),IFORB(2)
     1,X(2),XTENT(2),XPREV(2),XFAST(2),XSEC(2),XD(F(2)
      DIMENSION DATA(400)
      COMMON DUMMY(20,20)
      EQUIVALENCE(DUMMY(1),DATA(1))
      M=20
      NUSD1=20
      NUSD2=20
      N9=0
      DO 11 I=1,M
      DO 23 J=1,N
      N9=N9+1
   23 DATA(N9)=REAL(N(I,J))*1000000
   11 CONTINUE
      NUSD(1)=NUSD1
      NUSD(2)=NUSD2
      CTR=CSEG
C     ZERO THE MARK BITS OF EVERY DATUM
      I2MAX=(P14)*NUSD2
      DO 30 I1=1,NUSD1
      DO 30 I2=I1,I2MAX,NDIM1
C     ADDING 1.E-20 PREVENTS THE UNDERFLOW CAUSED BY BIT-MANIPULATIONS
      DATA(I2)=DATA(I2)+.E-20
   30 CALL ZERLO(DATA(I2))
      CTRZ=CTR*1.E-20
      CALL ZERLO(CTRZ)
      CTRM=CTRZ
```

```
      CALL MRKLD(CTPB,1,0.)
C     EPS IS CHOSEN LARGER THAN THE EFFECT OF ALTERING THE LOW ORDER BIT
      EPS=0.02
C     ***************************************************************
C     SEARCH FOR STARTING POINT FOR EACH CONTOUR AT HEIGHT CTR
      DO 390 I1=1,NUSD1
      DO 390 I2=1,NUSD2
      IPHAS=1
      CTRD=CTRZ
      IDIR=1
      XPREV(2)=-1.
      X(2)=0.
      IDELT(1)=1
      IDELT(2)=1
      IB(1)=I1
      IB(2)=I2
C     CHECK FOR EITHER A ROW CROSSING OR A COLUMN CROSSING
      DO 40 IVARY=1,2
      IF(IB(IVARY)-1) 40,40,30
30    IA(IVARY)=IB(IVARY)-1
      IUNVY=3-IVARY
      IA(IUNVY)=IB(IUNVY)
      GO TO 50
40    CONTINUE
      GO TO 390
C     ***************************************************
C     INTERNAL SUBROUTINE TO DETERMINE WHETHER THE SEGMENT FROM
C     (IA(1),IA(2)) TO (IB(1),IB(2)) IS CROSSED AND HAS NOT BEEN
C     PLOTTED ALREADY. A CROSSING IF FOUND IS AT (XTENT(1),XTENT(2)).
50    LA=IA(1)+NDIM1*(IA(2)-1)
      LB=IB(1)+NDIM1*(IB(2)-1)
      IF(DATA(LA)-CTRD)60,80,70
60    IF(DATA(LB)-CTRD) 120,80,80
70    IF(DATA(LB)-CTRD)80,80,120
80    IF(ABS(DATA(LA)-DATA(LB))-(CTRM-CTRZ))120,120,90
90    XTENT(IVARY)=FLOAT(IA(IVARY))+(FLOAT(IDELT(IVARY))*
     1(CTRD-DATA(LA)))/(DATA(LB)-DATA(LA))
      XTENT(IUNVY)=IA(IUNVY)
C     HAS THIS TENTATIVELY FOUND CROSSING BEEN PLOTTED BEFORE
      LX=IFIX(XTENT(1)+EPS)+NDIM1*IFIX(XTENT(2)+EPS-1.)
      RR=DATA(LX)
      IN=0
      CALL INMLO(IN,RR,IVARY)
      IF(IN)130,130,100
C     YES,BUT PERHAPS IT BE CAN BE PLOTTED AGAIN TO END A CONTOUR
100   IF(IPHAS-3)120,110,120
110   IF(ABS(XTENT(1)-XPREV(1))+ABS(XTENT(2)-XPREV(2))-EPS)120,120,130
120   IF(IPHAS-1)40,40,300
C     ***************************************************
C     PLOT AND MARK THE CURRENT CROSSING OR LABEL
130   IF(XPREV(2))140,150,160
C     SAVE THE FIRST AND SECOND CROSSINGS FOR REVERSE DIRECTION SEARCH
140   XFRST(1)=XTENT(1)
      XFRST(2)=XTENT(2)
      GO TO 170
150   XSEC(1)=XTENT(1)
      XSEC(2)=XTENT(2)
```

```
      XPRV(1)=X(1)
      XPRV(2)=X(2)
      X(1)=XIENT(1)
      X(2)=XIENT(2)
      IF(IDIR)190,190,190
  180 CALL CPLOT(IPHAS/4,XPRST(1),XPRST(2),CTP)
      IDIR=0
  190 CALL CPLOT(IPHAS/2,X(1),X(2),CTP)
      GO TO (200,210,350,380,390),IPHAS
  200 IPHAS=2
  210 DO 220 I=1,2
      IX(I)=X(I)+EPS
      XDIF(I)=X(I)-FLOAT(IX(I))-EPS
  220 IFORB(I)=(IX(I)+NUSD(I)-4)/(NUSD(I)-2)-1
      IF(IDIR)240,230,230
  230 LX=IX(1)+NDIM1*(IX(2)-1)
C     BOTH DIRECTIONS ARE MARKED IF THE CONTOUR PASSES THRU THE CORNER
      CALL MRKLOC(DATA(LX),IVARY,XDIF(IVARY))
C     ******************************************************************
C     LOOK IN ALL EIGHT POSSIBLE DIRECIONS FROM THE CURRENT CROSSING
C     FOR ANOTHER CROSSING.LOOK IN THE CURRENT DIRECTION FIRST,AT
C     ADJACENT SEGMENTS TO PREVENT FIGURE EIGHTS.
  240 IVARY=3-IVARY
      IVPRV=IVARY
      DO 330 LOOK=1,8
      DO 290 IVORY=1,2
      IF(XDIF(IVORY))250,250,270
C     IGNORE SEGMENTS OUTSIDE DATA OR WHICH INCLUDE THE CURRENT CROSSING
  250 IF(IDELT(IVORY)-IFORB(IVORY))260,300,260
  260 IB(IVORY)=IX(IVORY)+IDELT(IVORY)
      GO TO 290
  270 IF(IDELT(IVORY)+1-IVARY+IVORY)280,300,280
  280 IB(IVORY)=(X(IVORY)+(IDELP(IVORY)+1)/2
  290 IA(IVORY)=IB(IVORY)
      IA(IVARY)=IA(IVARY)-(IDELT(IVARY)
      IVARY=3-IVARY
      GO TO 50
  300 IDELP(IVPRV)=-IDELT(IVPRV)
      GO TO(310,311,310,320,330,310,330,320),LOOK
  310 IVARY=3-IVARY
      GO TO 330
  320 IVPRV=3-IVPRV
      IDELT(IVPRV)=-IDELT(IVPRV)
  330 CONTINUE
C     ******************************************************************
C     END THIS CONTOUR SEGMENT IF ALL DIRECTIONS FROM HERE HAVE BEEN
C     SEARCHED, AT MOST ONE CONNECTING POINT ON A LABEL IS NOW PLOTTED.
      IF(IPHAS-2)340,340,360
C     TRY CLOSING THE CONTOUR TO A NEARBY(EXCEPT THE PREVIOUS)CROSSING
  340 IPHAS=3
      CTP=CTPR
      GO TO 200
C     WRITE A CONTOUR LABEL AT THE END OF THIS CONTOUR
  350 LOOK=1
      IF(IDIR)390,390,360
C     JOIN THE CONTOUR CLOSE ON ITSELF(E.G.,A ONE-POINT CONTOUR)
  360 IF(ABS(X(1)-XPRST(1))+ABS(X(2)-XPRST(2))-EPS)370,370,390
```

```
370   IPHAS=5
      IF(YCPRV(2))180,180,190
C     IF THE CONTOUR HAS NOT CLOSED ON ITSELF,RETURN TO THE STARTING
C     POINT AND SEARCH FOR CONTINUATION IN ANOTHER DIRECTION
380   IPHAS=2
      CPRD=CTRZ
      IDIR=-1
      X(1)=XFRST(1)
      X(2)=XFRST(2)
      XPREV(1)=XSEC(1)
      XPREV(2)=YSEC(2)
      GO TO 210
390   CONTINUE
C     ***************************************************************
      IF(CSTP)400,410,400
400   CTR=CTR+SIGN(CSTP,CLIM-CBEG)
      IF((CTR-CLIM)*SIGN(1.,CLIM-CBEG)-.001*ABS(CSTP))10,10,410
C     IN CASE SUBROUTINE CPLOT IS SAVING UP POINTS,CLEAR IT OUT
410   CALL CPLOT(0,1.,1.,0.)
      RETURN
      END
      SUBROUTINE ZERLO(AIDATA)
C     SET THE TWO LOW ORDER BITS OF IDATA TO ZERO
C     IBM 360 REAL*4 OR INTEGER*4.
      IX=IFIX(AIDATA)
1     CONTINUE
      IF(IX) 30,21,30
30    IX=4*(IX/4)
      AIDATA=FLOAT(IX)
21    AIDATA=FLOAT(IX)
20    RETURN
      END
      SUBROUTINE IFNLO(IX,IIDATA,IVARY)
C     RETURN 0 IF BIT IVARY (=1 OR 2) OF IIDATA IS 0,1 IF NOT.
      IT=IIDATA
      RDATA4=(IT-4*(IT/4))
      IMX=IFIX(RDATA4)
      IF(IVARY.EQ.1) GO TO 70
      IF(IVARY.EQ.IMX) GO TO 20
      IX=0
      GO TO 30
20    IX=1
30    RETURN
      END
      SUBROUTINE ARKLO(CIDATA,IVARY,DIF)
C     SET BIT IVARY(=1 OR 2) OF IDATA TO 1. (TO BE CALLED ONLY ONCE
C     PER POINT). SET BOTH LOW ORDER BITS TO 1 IF DIF =0.
C     IBM 360 REAL*4 OR INTEGER*4
      IT=IFIX(CIDATA)
      IF(DIF)20,10,20
10    CIDATA=CIDATA+3-IVARY
20    RETURN
      END
      SUBROUTINE CPLOT(IPLOT,X1,X2,CTR)
      IF(IPLOT-10) 40,30,45
30    CALL LINE(X1,X2,IPLOT)
      GO TO 45
```